Manuscript Details

Manuscript number	FOODHYD_2020_222
Title	Potential of the encapsulation of oregano essential oil/α- and γ-cyclodextrin inclusion complexes into poly(3-hydroxybutyrate-co-3-hydroxyvalerate) films by electrospinning in the development of bioactive food packaging
Article type	Research paper

Abstract

Oregano essential oil (OEO) has good antioxidant and antimicrobial activity and its incorporation into food packaging is challenging because of its intense flavor, high volatility and instability, and insolubility in aqueous systems. Additionally, the sensory perception of EO can be changed as a consequence of oxidation, heating, volatilization or chemical interactions. Cyclodextrins (CDs) can be used to avoid these inconveniences because they are able, due to their peculiar chemical structure, to encapsulate hydrophobic molecules such as OEO improving its aqueous solubility and reducing its volatility. In this work, kneading (KM) and freeze-drying (FDM) methods were evaluated to encapsulate OEO in two cyclodextrins types (α-CD and γ-CD). After, the α-CD:OEO and γ-CD:OEO inclusion complexes (ICs) were included in poly(3-hydroxybutyrate-co-3-hydroxyvalerate) (PHBV) electrospun fibers by electrospinning and annealed for film formation. Results showed that the encapsulation efficiency of oregano essential oil is influenced by both the encapsulation methods and the cyclodextrin type. The antimicrobial and antioxidant activity of the α-CD:OEO and γ-CD:OEO inclusion complexes were higher compared with pure OEO. The optimal concentration of α-CD:OEO inclusion complexes and γ-CD:OEO inclusion complexes for homogeneous and continues films formation was 15 and 25 wt%, respectively. At these concentrations, the films showed a strong antimicrobial and antioxidant activity, up to 15 days. In addition, the mechanical properties of the films were also improved (Young's modulus + 35%). In conclusion, this work shows that the encapsulation of CD:OEO inclusion complexes by electrospinning into PHBV polymeric matrix opens a new path in the development of bioactive packaging materials using EOs.

Keywords	poly(3-hydroxybutyrate-co-3-hydroxyvalerate); cyclodextrins; oregano essential oil; antioxidant; antibacterial.

Corresponding Author	DANIELA ENESCU
Corresponding Author's Institution	INERNATIONAL IBERIAN NANOTECHNOLOGY LABORATORY
Order of Authors	DANIELA ENESCU, Kelly Johana Figueroa López, Jose Maria LAGARON, Lorenzo Pastrana, Pablo Fuciños, Sergio Torres-Giner, Luis Cabedo, Miquel Cerqueira
Suggested reviewers	Seonghyuk Ko, Orietta Monticelli, David Julian McClements, Hamid Mohammadi

Submission Files Included in this PDF

File Name [File Type]

Cover Letter.docx [Cover Letter]

HIGHLIGHTS.docx [Highlights]

Graphical Abstract.docx [Graphical Abstract]

text.docx [Manuscript File]

Captions.docx [Figure]

Fig 1.docx [Figure]

Figs 2.docx [Figure]

Fig 3.docx [Figure]

Figure 4.docx [Figure]

Figure 5.docx [Figure]

Figure 6.docx [Figure]

Figure 7.docx [Figure]

Figure 8.docx [Figure]

Figure 9.docx [Figure]

Figure 10.docx [Figure]

Figure 11.docx [Figure]

Table 1.docx [Table]

Table 2.docx [Table]

Table 3.docx [Table]

Table 4.docx [Table]

Table 5.docx [Table]

Table 6.docx [Table]

Table 7.docx [Table]

Conflict of Interest.docx [Conflict of Interest]

To view all the submission files, including those not included in the PDF, click on the manuscript title on your EVISE Homepage, then click 'Download zip file'.

Dear Editor Williams,

I submit in your attention the manuscript entitle

*"**Potential of the encapsulation of oregano essential oil / α- and γ-cyclodextrin inclusion complexes into poly(3-hydroxybutyrate-co-3-hydroxyvalerate) films by electrospinning in the development of bioactive food packaging**"*

authors: K. J. Figueroa-Lopez , D. Enescu, S. Torres-Giner, L. Cabedo, M. A. Cerqueira, L. Pastrana, P. Fuciños, J.M. Lagaron, to be published in Food Hydrocolloids.

I mention that the above manuscript has not been published elsewhere. Submitted manuscript is a research article.

Sincerely,
Daniela Enescu

HIGHLIGHTS

- Electrospinning of cyclodextrin:oregano essential oil inclusion complexes into poly(3-hydroxybutyrate-*co*-3-hydroxyvalerate) polymeric matrix was studied for the first time.
- The new packaging material revealed a good antimicrobial and antioxidant activity, up to 15 days.
- The Young's modulus of the new packaging material was increased up to 35%.

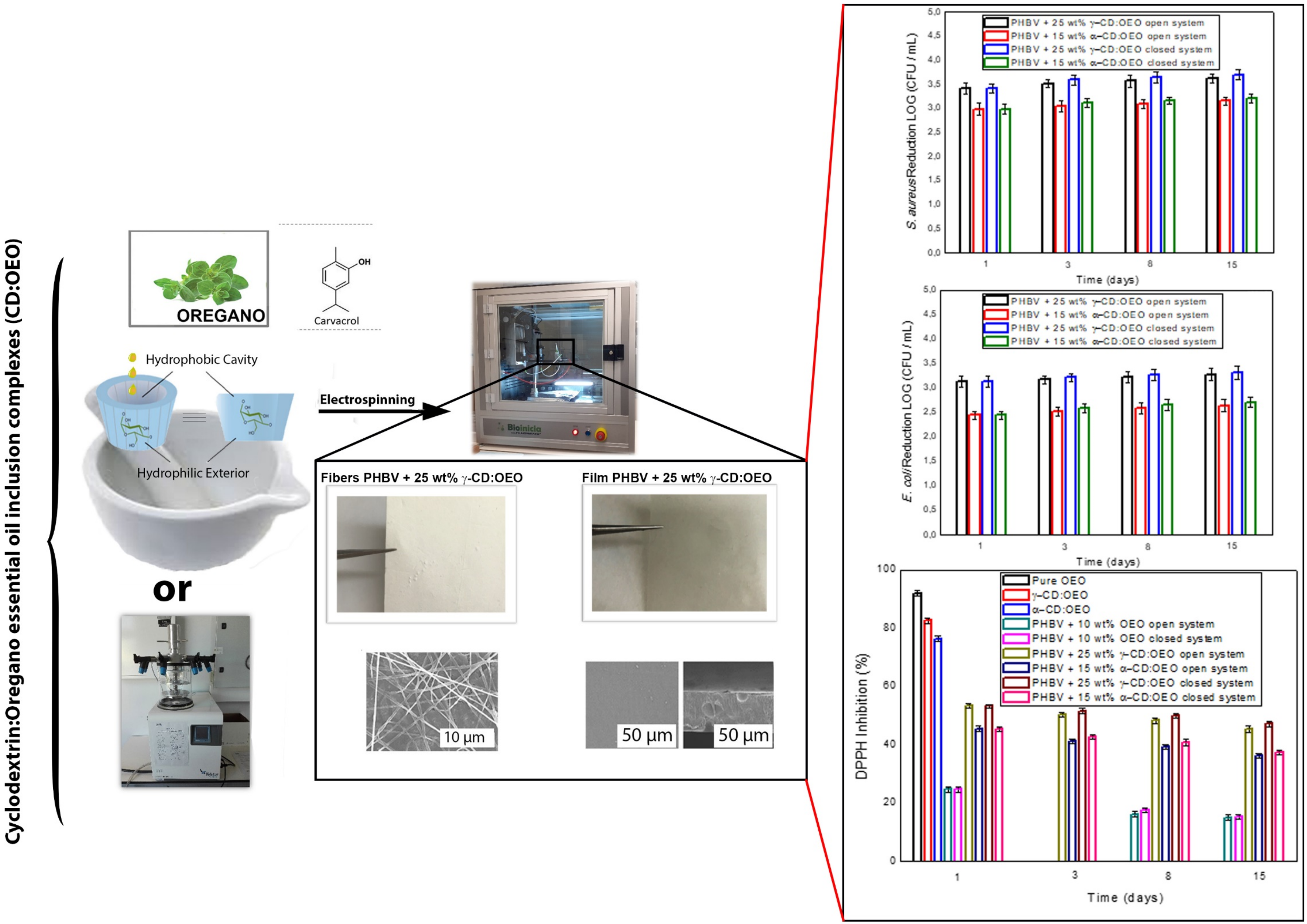

Cyclodextrin:Oregano essential oil inclusion complexes (CD:OEO)
OREGANO
Carvacrol
OH
Hydrophobic Cavity
Hydrophilic Exterior
or
Electrospinning
Bioinicia
Fibers PHBV + 25 wt% γ-CD:OEO
Film PHBV + 25 wt% γ-CD:OEO
10 µm
50 µm
50 µm
PHBV + 25 wt% γ-CD:OEO open system
PHBV + 15 wt% α-CD:OEO open system
PHBV + 25 wt% γ-CD:OEO closed system
PHBV + 15 wt% α-CD:OEO closed system
S. aureus Reduction LOG (CFU / mL)
E. coli Reduction LOG (CFU / mL)
Time (days)
Pure OEO
γ-CD:OEO
α-CD:OEO
PHBV + 10 wt% OEO open system
PHBV + 10 wt% OEO closed system
DPPH Inhibition (%)

Potential of the encapsulation of oregano essential oil/α- and γ-cyclodextrin inclusion complexes into poly(3-hydroxybutyrate-*co*-3-hydroxyvalerate) films by electrospinning in the development of bioactive food packaging

K. J. Figueroa-Lopez [a*], D. Enescu[b**], S. Torres-Giner [a], L. Cabedo [c], M. A. Cerqueira [b], L. Pastrana [b], P. Fuciños [b], J.M. Lagaron [a***]

*Corresponding author. Novel Materials and Nanotechnology Group, Instituto de Agroquímica y Tecnología de Alimentos (IATA), Calle Catedrático Agustín Escardino Benllonch 7, 46980 Valencia, Spain; International Iberian Nanotechnology Laboratory (INL), Department Life Sciences, Research Unit: Nano4Food/Food Processing, Braga, Portugal

E-mail addresses: kjfigueroal@iata.csic.es (K.J. Figueroa-Lopez); danielaenescuu@gmail.com (D. Enescu), lagaron@iata.csic.es (J.M. Lagaron).

[a] Novel Materials and Nanotechnology Group, Instituto de Agroquímica y Tecnología de Alimentos (IATA), Calle Catedrático Agustín Escardino Benllonch 7, 46980 Valencia, Spain.

[b] INL - International Iberian Nanotechnology Laboratory, Av. Mestre José Veiga s/n, 4715-330, Braga, Portugal.

[c] Polymers and Advanced Materials Group (PIMA), Universitat Jaume I (UJI), Avenida de Vicent Sos Baynat s/n, 12071 Castellón, Spain.

ABSTRACT Oregano essential oil (OEO) has good antioxidant and antimicrobial activity and its incorporation into food packaging is challenging because of its intense flavor, high volatility and instability, and insolubility in aqueous systems. Additionally, the sensory perception of EO can be changed as a consequence of oxidation, heating, volatilization or chemical interactions. Cyclodextrins (CDs) can be used to avoid these inconveniences because they are able, due to their peculiar chemical structure, to encapsulate hydrophobic molecules such as OEO improving its aqueous solubility and reducing its volatility. In this work, kneading (KM) and freeze-drying (FDM) methods were evaluated to encapsulate OEO in two cyclodextrins types (α-CD and γ-CD). After, the α-CD:OEO and γ-CD:OEO inclusion complexes (ICs) were included in poly(3-hydroxybutyrate-co-3-hydroxyvalerate) (PHBV) electrospun fibers by electrospinning and annealed for film formation. Results showed that the encapsulation efficiency of oregano essential oil is influenced by both the encapsulation methods and the cyclodextrin type. The antimicrobial and antioxidant activity of the α-CD:OEO and γ-CD:OEO inclusion complexes were higher compared with pure OEO. The optimal concentration of α-CD:OEO inclusion complexes and γ-CD:OEO inclusion complexes for homogeneous and continues films formation was 15 and 25 wt%, respectively. At these concentrations, the films showed a strong antimicrobial and antioxidant activity, up to 15 days. In addition, the mechanical properties of the films were also improved (Young's modulus + 35%).

In conclusion, this work shows that the encapsulation of CD:OEO inclusion complexes by electrospinning into PHBV polymeric matrix opens a new path in the development of bioactive packaging materials using EOs.

HIGHLIGHTS

- Electrospinning of cyclodextrin:oregano essential oil inclusion complexes into poly(3-hydroxybutyrate-*co*-3-hydroxyvalerate) polymeric matrix was studied for the first time.
- The new packaging material revealed a good antimicrobial and antioxidant activity, up to 15 days.
- The Young's modulus of the new packaging material was increased up to 35%.

***Keywords**:* poly(3-hydroxybutyrate-co-3-hydroxyvalerate), cyclodextrins, oregano essential oil, antioxidant, antibacterial.

1. Introduction

Essential oils (EOs) are mixtures of volatile organic compounds obtained from aromatic plants that are well known for their fragrant properties. They are also used in food preservation and in antimicrobial, analgesic, sedative, anti-inflammatory, spasmolytic and locally anesthetic remedies (Bakkali, Averbeck, Averbeck, & Idaomar, 2008; Ribeiro-Santos, Andrade, Melo, & Sanches-Silva, 2017). Their mechanisms of active and bioactive action, particularly at the antimicrobial level, have been well reported (Owen & Laird, 2018; Sharifi-Rad et al., 2017). The global market of EOs was 226.9 kton/year in 2018 (Research, 2018) while approximately 160 essential oils are considered as Generally Recognized as Safe (GRAS) by the U.S. Food and Drug Administration (FDA, 2016). Therefore, their application is currently growing in the food and beverage, personal care & cosmetics, aromatherapy, and pharmaceutical industries (Bakhtiary, Sayevand, Khaneghah, Haslberger, & Hosseini, 2018; Prakash, Kedia, Mishra, & Dubey, 2015; Prakash, Singh, Kedia, & Dubey, 2012; Raut & Karuppayil, 2014).

Among EOs, oregano essential oil (OEO) is one of the most interesting since it is FDA approved and it is also included by the Council of Europe in the list of chemical flavorings that may be added to foodstuffs (EU No 872/2012; De Vincenzi, Stammati, De Vincenzi, & Silano, 2004). In particular, OEO contains a mixture of bioactive related components such as carvacrol and thymol that can be used as antioxidant and antimicrobial agents for active packaging purposes (Figueroa-Lopez, Vicente, Reis, Torres-Giner, & Lagaron, 2019). However, the incorporation of OEO into a food packaging material is a challenging task due to several factors such as potent flavor changes, variations of the sensory perception as a consequence of oxidation, high volatility, chemical instability, low solubility in aqueous systems, etc. (Ju et al., 2019). In particular, OEO can evaporate easily and it decomposes and oxidizes during formulation, processing, and storage due to exposure to heat, pressure, light, or oxygen (Beirão-da-Costa et al., 2013; Hosseini, Zandi, Rezaei, & Farahmandghavi, 2013). These inconveniences can be effectively minimizing by encapsulation processes in different systems such as films, capsules, liposomes or inclusion complexes (Crini, 2014; Marques, 2010; Sherry, Charcosset, Fessi, & Greige-Gerges, 2013). Encapsulation allows creating a physical barrier between the core and the wall materials to protect OEO from the external medium (moisture, heat, light) and, thus, it enhances stability and maintains bioactivity (Sagiri, Anis, & Pal, 2016).

Cyclodextrins (CDs) are cyclic oligosaccharide consisting of six, that is, α-cyclodextrin (α-CD), seven, that is, β-cyclodextrin (β-CD) or eight, that is, γ-cyclodextrin (γ-CD) glucopyranose units modified starch molecules shaped like a hollow truncated cone (Del Valle, 2004). CDs are fairly water soluble, however β-CD shows remarkably lower solubility than α-CD and γ-CD. During crystallization in aqueous medium, some molecules of water are entrapped into the CD cavity whereas others molecules of water are present as integral parts of the crystal structure, the so-called crystal water. CD inclusion complexes are formed by the substitution of the water molecules of the CD cavity by the appropriate guest molecule (Harada, Suzuki, Okada, & Kamachi, 1996; Szejtli, 1998). These inclusion complexes can be used to encapsulate different compounds since CDs cannot only stabilize the compound encapsulated against the degradation mechanisms triggered by environmental conditions but they also can reduce the sensory changes by masking strong flavors (Marques, 2010; Szejtli, 1998). Furthermore, CDs can also offer a controlled and sustained release of aromatic substances (Marques, 2010; Wang & Chen, 2005). In addition, the CD chemical structures are habitually inert and they do not interfere with the biological properties of EOs (Bilia et al., 2014; Del Valle, 2004). They are additionally relatively cost effective, biodegradable, do not pose a significant safety concern, and encapsulation can be performed both in solution and solid state (Crini, 2014). Several procedures have been then developed to prepare inclusion complexes, for instance kneading method (KM), co-precipitation, heating in a sealed container, freeze-drying method (FDM), spray drying, and supercritical fluid technology (Loftsson & Brewster, 1996). The essentials oils are thermolabile substances sensitive to the effects of light, oxygen, humidity and high temperatures and can be lost activity. It is for this reason that the electrospinning encapsulation technology has been used for the protection, stabilization, solubilization and delivery of the active substances (Gao et al., 2019).

In this regard, the electrospinning process is a novel technology that produces ultrathin fibrous mats made of a wide range of polymers and biopolymers with fiber diameters ranging from several nanometers to a few microns (Li & Xia, 2004). This technique is highly suitable for the nanoencapsulation of active and bioactive substances, which is the case of CDs, due to both the high surface-to-volume ratios of the electrospun materials and the high porosity of their mats (Torres-Giner, Pérez-Masiá, & Lagaron, 2016; Torres-Giner, Wilkanowicz, Melendez-Rodriguez, & Lagaron, 2017). Furthermore, allow processing volatile substances such as CDs because the process is performed at room temperature (Kayaci & Uyar, 2012). The resultant electrospun fibers can be potentially applied in sustainable food packaging applications (Torres-Giner, 2011; Torres-Giner, Busolo, Cherpinski, & Lagaron, 2018) either in the form of coatings or interlayers with bioplastic films (Quiles-Carrillo, Montanes, Lagaron, Balart, & Torres-Giner, 2019a; Torres-Giner, Martinez-Abad, & Lagaron, 2014). Moreover, the electrospun mats can be subjected to a thermal post-treatment, also called annealing, by which they form mechanically strong and transparent films with little porosity due to the fibers coalescence (Cherpinski, Torres-Giner, Cabedo, & Lagaron, 2017). Due to the advantages described above, electrospinning has been recently employed to produce multi-functional fibers from different biopolymers (Gao et al., 2019), such as polyhydroxyalkanoates (PHAs), that are biodegradable microbial polyesters (Zhang, Shishatskaya, Volova, da Silva, & Chen, 2018). Indeed, PHAs are excellent candidates for food packaging applications due to their resistance to water, low oxygen permeability, thermoplastic processability, and good physical and mechanical properties (Dietrich, Dumont, Del Rio, & Orsat, 2019).

In this context, the aim of this research work was to encapsulate oregano essential oil into cyclodextrins and their inclusion into poly(3-hydroxybutyrate-*co*-3-hydroxyvalerate) (PHBV) fibers by electrospinning to develop an active packaging material with improved antioxidant and antimicrobial activity to design biodegradable packaging that can prolong the shelf life of certain food products.

2. Experimental

2.1. Materials

Oregano essential oil (OEO) with a purity >99% and a density of 0.925–0.955 g/mL was obtained from Gran Velada S.L. (Zaragoza, Spain) and it was processed as received. Wacker Chemie AG (Munich, Germany) supplied both food-grade cyclodrextin (CD): α-CD, known as trademark - CAVAMAX® W6 FOOD with molecular (M_W) of 972.84 g/mol and γ-CD, known as trademark - CAVAMAX® W8 FOOD with M_W of 1297 g/mol. Their respective empirical formulas were $C_{36}H_{60}O_{30}$ and $C_{48}H_{80}O_{40}$ while the chemical structures are shown in Fig. 1 and further details are gathered in Table 1. Commercial PHBV was ENMAT™ Y1000P, produced by Tianan Biologic Materials (Ningbo, China) and delivered in the form of pellets by Nature Plast (Ifs, France). According to the manufacturer, this biopolymer resin presents a density of 1.23 g/cm^3 and a melt flow index (MFI) of 5–10 g/10 min (190 ºC, 2.16 Kg). The 3HV fraction in the copolyester is 2–3 mol.-%. 2,2,2-trifluoroethanol (TFE), ≥99% purity and 2,2-diphenyl-1-picrylhydrazyl radical (DPPH) were purchased from Sigma Aldrich S.A. (Madrid, Spain). Ethanol, analytical grade with purity of 99.8%, was supplied by Sigma-Aldrich. Water Milli-Q® was obtained using a Millipore purification system (resistivity □ 18.2 MΩ·cm at 25 ºC).

Table 1

Fig. 1

Preparation of the Inclusion Complexes

To prepare the inclusion complexes, OEO was dispersed in CD aqueous solutions at the weight ratios of 20:80 wt/wt and 15:85 wt/wt for γ-CD and α-CD, respectively. These weight ratios between guest:host (OEO:CD) were chosen based on the maximum encapsulation efficiency reported by (Petrovi, Stojanovi, & Radulovi, 2010) and (Haloci et al., 2014).

2.2.1. Kneading Method (KM)

The inclusion complexes was carried out by KM as described by (Santos, Kamimura, Hill, & Gomes, 2015) and (Hedges, 1998) with some modifications. Briefly, OEO was dispersed in the CD aqueous solutions and water was added at 0.25 mL. The resultant CD:OEO mixture was kneaded thoroughly in a mortar and pestle for 18 min until a homogenous blend was obtained. The kneaded inclusion complexes (pasty mass) obtained was dried in a desiccator under vacuum for 48 h at room temperature (25 ºC) and then weighted, sealed, and stored at -20 ºC.

2.2.2. Freeze Drying Method (FDM)

The preparation of the inclusion complexes by the FDM was carried out according to (Santos et al., 2015) with also slight modifications. OEO was dispersed in 2.5 ml of the CD aqueous solutions and the resultant mixtures were magnetically stirred at 250 rpm in a sealed container for 48 h at room temperature (25 ºC) to allow complex formation. Paraffin film and aluminium foil was used to prevent loss of volatiles and to protect the samples from the light. The suspensions were then frozen first at -20 ºC for 24 h and then at -80 ºC for 24 h and finally lyophilized at -50 ºC and 0.1 mbar in a Freeze Dryer (LyoQuest -55 Plus Eco Telstar® Life Science solutions, Hampton, USA) until the water was sublimated (approximately 48 h). The freeze-dried inclusion complex was weighted, sealed, and stored at -20 ºC.

2.3. Inclusion Complexes Characterization

2.3.1. Entrapment Efficiency and Loading Capacity

10 mg of each type of inclusion complexes (α-CD:OEO and γ-CD:OEO at 80:20 and 15:85 weight ratios), were dispersed in 10 mL of absolute ethanol and stirred for 30 min in an Eppendorf mixer device (ThermoMixer™ C, Fisher Scientific®, Hampton, USA) at 1000 rpm to allow the entrapped OEO in the CD cavity to be released to the solution for analysis. Then, the solution obtained was sonicated in a ultrasonic bath for 30 min at 37 Hz and 90 W at room temperature and thereafter centrifugated for 30 min at 2500 rpm to remove any CD from the solution. This resulted in a solution with a supernatant containing the OEO, which was used for analysis. The OEO content was determined spectrophotometrically (Ultraviolet-Visible spectrophotometer, UV-VIS 2250, Shimadzu) monitoring the absorbance at wavelength 275 nm. This wavelength absorption belongs to the maximum absorbance wavelength of carvacrol, which is the most representative compound and major component of OEO (Santos et al., 2015). From this wavelength absorption, the mass of the encapsulated OEO in the absolute ethanol solutions was calculated. A calibration curve of the absorbance versus the concentration of the OEO was previously performed by using OEO solutions of known concentrations dissolved in ethanol.

The encapsulation efficiency (EE, %) and loading capacity (LC, %), for each sample, were calculated according to Equations (1) and (2), respectively (Santos, et al. 2015). Encapsulation efficiency (EE, %) is the encapsulated amount of essential oil expressed as a percentage of the quantity initially used to prepare the solid inclusion complex. The UV-VIS analysis was carried out in triplicate.

$$\text{Encapsulation Efficiency (\%)} = \frac{\text{Total amount of encapsualted essential oil (mg)}}{\text{Initial amount of essential oil to be encapsulated (mg)}} \times 100\ (\%) \qquad (1)$$

$$\text{Loading Capacity (\%)} = \frac{\text{Total amount of encapsualted essential oil (mg)}}{\text{Total amount of ICs (mg)}} \times 100\ (\%) \qquad (2)$$

2.3.2. Morphological characterization of CD:OEO inclusion complexes

The morphology of empty CDs and CD:OEO inclusion complexes were examined using a scanning electron microscope (FEI Quanta 650 FEG, Thermo Fisher Scientific®, Germany). The samples were fixed on aluminium stubs with a double-stick conductive carbon substrate and sputter-coated with gold for 63 s at a working pressure of 1.4 E^{-3} mbar before the SEM measurements to prevent the build-up of an electric negative charge in the specimen, which would induce "imaging artefacts" and to enhance resolution. Observations were carried out with voltage acceleration of 10 kV and15 kV at spot 3. Transmission Electron Microscopy (TEM) was also used. Droplets of 0.1 % (w/v) and 1 % (w/v) aqueous suspensions (i.e. empty "*as-received*" α-CD and γ-CD; α-CD:OEO and γ-CD:OEO inclusion complexes) were placed on a copper grid and air-dried overnight. For negative staining, one drop of UranyLess 22409 was used. Observations were carried out with voltage acceleration of 200 kV at α_3, spot 1 and magnification: 30KX-100KX (JEOL JEM 2100, Izasa Scientific®, Portugal). The X-ray diffractograms of empty α-CD and γ-CD; α-CD:OEO and γ-CD:OEO inclusion complexes were obtained using a X-ray diffractometer (PANalitycal X'pert MPD-PRO (PANalytical, Model: X PERT PRO MRD) Bragg-Brentano θ-θ geometry using CuKα radiation at 45kV and 40 mA. The 2θ scan range was 5° - 80° with a step size of 0.01° and a time/step of 0.5 s.

2.4. Electrospinning Process

2.4.1. Preparation of Solutions

A PHBV solution for electrospinning was prepared by dissolving 10 % of biopolymer in TFE (wt/vol) at room temperature. The γ-CD:OEO and α-CD:OEO inclusion complexes were incorporated into the PHBV solution at 10, 15, 20, 25 and 30 wt% in relation to the biopolymer. PHBV solutions with γ-CD and α-CD (25 and 15 wt%, respectively), without OEO, were also prepared as a control sample.

2.4.2. Electrospun Fibers

The PHBV solutions containing γ-CD:OEO and α-CD:OEO were electrospun using a high-throughput electrospinning/electrospraying pilot line Fluidnatek® LE 500 manufactured and commercialized by Bioinicia S.L. (Valencia, Spain). The solutions were processed under a constant flow using a 24 emitter multi-nozzle injector, scanning vertically onto a flat slightly negatively charged collector. A voltage difference of 18 kV, a flow-rate of 6 mL/h per single emitter, and a tip-to-collector distance of 20 cm were used as these were the most optimal conditions (Melendez-Rodriguez et al., 2019).

2.4.3. Electrospun Films

An annealing treatment was thereafter applied to the electrospun mats in a 4122-model press from Carver, Inc. (Wabash, IN, USA) at 160 ºC, for 10 seconds, without pressure. These conditions were selected based on our previous study (Melendez-Rodriguez et al., 2019). The resultant film samples had an average thickness of approximately 80 µm.

2.4.4. Characterization of the Electrospun Films

2.4.4.1. Film Thickness

Before testing, the thickness of all films was measured using a digital micrometer (S00014, Mitutoyo, Corp., Kawasaki, Japan) with ± 0.001 mm accuracy. Measurements were performed and averaged in five different points, two in each end and one in the middle.

2.4.4.2. Morphology

The particle shape and size (diameter) distributions of γ-CD and α-CD, the PHBV electrospun fibers and their films containing γ-CD:OEO and α-CD:OEO were examined by scanning electron microscopy (SEM; Hitachi S-4800, Tokyo, Japan) and transmission electron microscopy (TEM; Hitachi HT7700, Tokyo, Japan). For cross-section observations by SEM, the films were previously cryo-fractured by immersion of the sample in liquid nitrogen. The SEM micrographs were taken at an accelerating voltage of 10 kV and a working distance of 8 – 10 mm, the samples were previously sputtered with a gold□palladium mixture for 3 min under vacuum. The size distribution of the particles and average fibers diameter was determined via ImageJ software using at least 20 SEM images.

2.4.4.3. Transparency

The light transmission of the films was determined in specimens of 50 x 30 mm^2 by quantifying the absorption of light at wavelengths between 200 nm and 700 nm, using an UV–Vis spectrophotometer VIS3000 from Dinko, Instruments (Barcelona, Spain). The transparency value (T) was calculated using Equation 3 (K. Figueroa-Lopez, Andrade-Mahecha, & Torres-Vargas, 2018):

$$T = \frac{A_{600}}{L} \quad (3)$$

Where A_{600} is the absorbance at 600 nm and L is the film thickness (mm).

2.4.4.4. Thermal Analysis

Thermogravimetric analysis (TGA) of the γ-CD, α-CD, films containing γ-CD:OEO and α-CD:OEO was performed under nitrogen atmosphere in a Thermobalance TG-STDA Mettler Toledo model TGA/STDA851e/LF/1600 analyzer. TGA curves were obtained after conditioning the samples in the sensor for 5 min at 30 °C. The samples were then heated from 25 °C to 700 °C at a heating rate of 10°C/min. First derivative of thermogravimetry (DTG) curves, expressing the weight loss rate as the function of time, were obtained using TA analysis software. All tests were carried out in triplicate.

2.4.4.5. Mechanical Tests

Tensile tests were performed according to ASTM Standard D 638 on an Instron Testing Machine (Model 4469; Instron Corp; Canton, MA, USA). The film samples were dumbbell-shaped. The cross-head speed was fixed at 10 mm/min. At least six samples were tested for each material and the average values of the mechanical parameters and standard deviations were reported. Tensile modulus (E), tensile strength at break (σ_b), and elongation at break (ε_b) were calculated from the stress–strain curves, estimated from the force–distance data.

2.5. Antimicrobial Activity

Staphylococcus aureus CECT240 (ATCC 6538p) and *Escherichia coli* CECT434 (ATCC 25922) strains were obtained from the Spanish Type Culture Collection (CECT: Valencia, Spain) and stored in phosphate buffered saline (PBS) with 10 wt.% tryptic soy broth (TSB, Conda Laboratories, Madrid, Spain) and 10 wt.% glycerol at −80 ºC. Previous to each study, a loopful of bacteria was transferred to 10 mL of TSB and incubated at 37 ºC for 24 h. A 100 µL aliquot from the culture was again transferred to TSB and grown at 37 ºC to the mid-exponential phase of growth. The approximate count of 5 x 10^5 CFU / mL of culture having absorbance value of 0.20 as determined by optical density at 600 nm (UV–Vis spectrophotometer VIS3000 from Dinko, Instruments, Barcelona, Spain).

The minimum inhibitory concentration (MIC) and bactericide (MIB) values of γ-CD:OEO and α-CD:OEO against food-borne bacteria was tested following the plate micro-dilution protocol based on our previous work (Figueroa-Lopez et al., 2019). For this, a 96-well plate with an alpha numeric coordination system (columns 12 and rows A-H) were used, where 10 µl of the tested samples were introduced in the wells with 90 µl of the bacteria medium. In the wells corresponding to A, B, C, E, F, and G columns different concentrations of CD/OEO (0.039, 0.078, 0.156, 0.312, 0.625, 1.25, 2.5, 5, 10, 20 µg/mL), were tested, in triplicate, from rows 1 to 10. Columns D and H were used as control of CD:OEO in TSB without bacteria. Row 11 was taken as positive control, that is, only TSB, and row 12 was used as negative control, that is, *S. aureus* and *E. coli* in TSB. The plates were incubated at 37 °C for 24 h. Thereafter, 10 µl of resazurin, a metabolic indicator, was added to each well and incubated again at 37 °C for 2 h. Upon obtaining the resazurin change, the wells were read through color difference. The MIC value was determined as the lowest concentration of γ-CD:OEO and α-CD:OEO presenting growth inhibition.

The antimicrobial performance of the electrospun PHBV films containing γ-CD:OEO and α-CD:OEO was evaluated by using a modification of the Japanese Industrial Standard (JIS) Z2801 (ISO 22196:2007) (Figueroa-Lopez, Castro-Mayorga, Andrade-Mahecha, Cabedo, & Lagaron, 2018). A microorganism suspension of *S. aureus* and *E. coli* was applied onto the test films containing γ-CD:OEO and α-CD:OEO, films without CD:OEO (negative control) sizing 1.5 x 1.5 cm^2 that were placed in either open bottles. After incubation at 24 °C and at a relative humidity (RH) of at least 95 % for 24 h, bacteria were recovered with PBS, 10-fold serially diluted and incubated at 37 °C for 24 h in order to quantify the number of viable bacteria by conventional plate count. The antimicrobial activity was evaluated from 1 (initial day), 8, and 15 days. The value of the antimicrobial activity (R) was calculated using Equation 4:

$$R = \left[Log\left(\frac{B}{A}\right) - Log\left(\frac{C}{A}\right)\right] = Log\left(\frac{B}{C}\right) \quad (4)$$

Where *A* is the average of the number of viable bacteria on the control sample immediately after inoculation, *B* is the average of the number of viable bacteria on the control sample after 24 h, and *C* is the average of the number of viable bacteria on the test sample after 24h. Three replicate experiments were performed for each sample and the antibacterial activity was evaluated with the following assessment: Nonsignificant ($R<0.5$), slight ($R \geq 0.5$ and <1), significant ($R \geq 1$ and <3), and strong ($R \geq 3$) (Sergio Torres-Giner, Torres, Ferrándiz, Fombuena, & Balart, 2017).

2.6. Antioxidant Activity

The DPPH inhibition assay was used to evaluate the free radical scavenging activity of the neat OEO, γ-CD:OEO, α-CD:OEO, and the electrospun PHBV films containing γ-CD:OEO and α-CD:OEO. Samples were weighed in triplicate in cap vials and then an aliquot of the DPPH solution (0.05 g/L in methanol) was added to each one. Vials without samples were also prepared as controls. All the samples were prepared and immediately stored at room temperature for 2 h in darkness. After this, the absorbance of the solution was measured at 517 nm in the UV 4000 spectrophotometer from Dinko Instruments. Results were expressed as the percentage of inhibition to DPPH following Equation 5 (Busolo & Lagaron, 2015) and µg equivalent of trolox per gram of sample, employing a previously prepared calibration curve of trolox.

$$Inhibition\ DPPH\ (\%) = \frac{A_{Control} - (A_{sample} - A_{blank})}{A_{control}} * 100 \quad (4)$$

Where $A_{control}$, A_{blank}, and A_{sample} are the absorbance values of the DPPH solution, methanol with the test sample, and the test sample, respectively.

2.7. Statistical Analysis

The results of the encapsulation efficiency and loading capacity of the CD:OEO inclusion complexes, mechanical test and antioxidant activity were evaluated by analysis of variance (ANOVA) and a multiple comparison test (Tukey) with 95% significance level (p □0.05). For this purpose, we used the software OriginPro8 (OriginLab Corporation, USA).

3. Results and discussions

3.1. Encapsulation Efficiency (EE,%) and Loading capacity (LC, %) of the CD:OEO Inclusion Complexes

The EE and LC of the α-CD:OEO and γ-CD:OEO inclusion complexes prepared by FDM and KM are presented in Table 2. The results show that both types of cyclodextrins (α-CD and γ-CD) are efficient wall materials for encapsulation of oregano essential oil presenting EE values ragging from 36.03 % to 98.5 % depending on the weight ratio (CDs:OEO) as well as on the preparation method. Indeed, by the FDM is obtained a lower encapsulation efficiency than by KM method, and this is in accordance with those described by Ozdemir et al. (2018), who studied the encapsulation of black paper oleoresin in β-cyclodextrin with encapsulation efficiencies from 90.2 % to 79.3 % for KM and FDM, respectively. The higher encapsulation efficiency obtained by KM compared to FDM can be related to the high shear rate applied (Ozdemir et al., 2018), and the use of low amount of water during the inclusion complex formation. In an aqueous solution, the cyclodextrin cavity is slightly polar and occupied by water molecules, and can therefore be readily replaced by appropriated guest molecules, that are less polar than water (Ponce Cevallos, Buera, & Elizalde, 2010). It is also worthy to mention that some differences in the EE values could be associated with evaporation of volatile components during the preparation process studies (Ozdemir et al., 2018; Santos et al., 2015). In conclusion, the preparation parameters of the α-CD:OEO and γ-CD:OEO inclusion complexes, that is, weight ratio host-guest, nature of cyclodextrin, use of co-solvent and its quantity, mixing time, and shear rate applied could affect the properties of the obtained complexes such as the encapsulation yield. Thus, based on the results obtained in terms of EE, KM revealed to be the most efficient method for the encapsulation of OEO in the CD cavity, and it also added value in terms of simplicity, rapidity, and the desired characteristics of the final product.

Table 2

3.2. Morphology of the CD:OEO Inclusion Complexes

The morphology of the CD:OEO inclusion complexes was observed by SEM and compared with the empty α-CD and γ-CD. The SEM images showed that the size and shape of the inclusion complex (Figs. 2b, 2d, 2e, 2f, 2g, 2h) are different of the empty α- and γ- CD (Figs. 2a, 2c, 2i, 2j) as it was confirmed at different magnifications. The shape of empty "*as-received*" α- and γ- CD appear uneven and the size range from 24 μm up to 254 μm; large particle sizes which seem to pile up thus forming large aggregates. The relative larger size of empty "*as-received*" α- and γ- CD could be attributed to the agglomeration of empty "*as-received*" α- and γ-CD particles via hydrogen bonding. In the absence of a guest molecule empty "*as-received*" α- and γ- CD tend to cluster and agglomerate due to lack of significant net charge on the particles, that is, no repulsive forces to prevent agglomeration (Hill, Gomes, & Taylor, 2013). This is also consistent with the observation of smaller particles attraction and adherence to the larger particles (*see* in detail in Figs. 2a, $2a_1$, $2a_2$ and 2c, $2c_1$, $2c_2$); similar observations were presented by Santos et al. (2015). Contrarily, this behaviour not occurs in the formed α-CD:OEO and γ-CD:OEO inclusion complexes; the reduction of the particle size in the α-CD:OEO and γ-CD:OEO inclusion complexes indicated a conformational change of empty α-CD and γ-CD that obstructed the agglomeration among them (Guimarães et al., 2015; Seo, Min, & Choi, 2010). Indeed, compared with empty "*as-received"* α- and γ- CD (i.e., particle size: 24 μm ÷254 μm; similar to that found by Gauret et. al. (2018), their inclusion complexes showed a remarkable decrease in particle size, range from ~5 μm up to nanometric level (~100 nm) and with well-defined lamella shaped (tetragonal crystals). In both types of inclusion complexes were observed lamella-like sheets and microrods (Figs. 2b and 2d).

Figs. 2a, 2b, 2c, 2d

In addition, the microrods from ICs had a very high aspect ratio (*see* Figs 2e and 2f). Observation over a large number of SEM images suggests that these long microrods stack together to produce the lamella-like sheets.

Figs. 2e and 2f

The morphology similarity of both types of α-/γ- CD: oregano essential oil inclusion complexes could be explained by considering the solubility of the used CDs (*see* Table 1). Saokham et al. (2018), and the referenced cited within exanimated why the solubility of α and γ is different towards β; briefly, γ-CD, which is the largest of the three, is the most soluble (23.20 mg/100 ml H_2O) while β-CD, which is in the intermediate, is the least soluble in water (1.8 g/100 ml H_2O). These differences in the solubility of the CDs are related to the way the CD glucose units are geometrically aligned with each other. It has been proposed that in the β-CD molecule, all the 7 glucose units lie in the same plane. Hence, in this arrangement, all the glucose primary hydroxyl groups at the CD narrower end are able to form hydrogen bonds with each other. At the same time, all the secondary hydroxyl groups at the wider CD opening form hydrogen bonds with each other. The hydrogen bonding below and above the ring leads to secondary belts which increases the rigidity of the β-CD and therefore causes low solubility. Contrary to, α- and γ- CD which do not have secondary belts therefore their structures are flexible, and are hence very soluble due to the availability of free hydroxyl groups. During trituration of cyclodextrins in aqueous medium, a few water molecules could entrap into the cyclodextrin cavity, whereas other molecules of water are present as integral parts of the crystal structure (crystal water). According to Rusa et al. (2002);

Szeijtli (1998); Das et al. (2015) the cyclodextrin - inclusion complexes are formed by the substitution of included water from cyclodextrin cavity by the appropriate guest molecule.

Using the above reasoning, the threading of oregano essential oil can occur faster in α-CD and γ- CD molecules than that with β-CD. Hence, the morphology similarity of both types of ICs (α-CD:OEO and γ-CD:OEO) studied in this work could be explained using the above reasoning. Moreover, the particle size distribution appears quite homogenous and have rather smooth and parallel surfaces (Figs. 2b, 2d, 2e, 2f, 2g, 2h). They all have sharp edges, as expected from crystalline structures. The growth of the crystals is definitely preferential in 2D (lamella-shape). Figs. 2g and 2h show other details: the two arrows point out the thickness, around a few hundreds of nm, of a platelet with a size of 100 nm - ~ 5µm. Smaller platelets (under 500 nm) appear to have the same thickness. These results show that the morphological characteristic of inclusion complexes are indeed different from empty "*as-received*" α-CD and γ- CD; empty "*kneaded for 18 minutes at R.T.*" α-CD and γ- CD, and empty"*kneaded for 18 minutes with 0.25 mL distilled water at R.T.*" α-CD and γ-CD. This morphological difference between the empty CDs and the inclusion complexes obtained is in agreement with the observations reported by Guimaraes et al. (2015), and the references cited within.

Figs. 2g, 2h, 2i, and 2j

To elucidate if the morphology, in terms of particle size and well-defined shape, of empty " *as-received*" α- and γ- CD was changed due to the encapsulation of essential oil (i.e. low particle size and well-definite lamella shape), was performed SEM also on empty "*kneaded for18 minutes at R.T.*" α- and γ- CD, and empty "*kneaded for 18 minutes at R.T. with 0.25 ml distilled water (the same quantity used at the preparation of inclusion complex)*" α- and γ- CD. The results showed that compared with empty "*as-receive*" α- and γ- CD there is not significant morphological modification after their kneaded for 18 minutes at R.T. (Figs. $2a_1$ and $2c_1$) as well as after their kneaded for18 minutes at R.T. with 0.25 ml distilled water (Figs. $2a_2$ and $2c_3$). The presence of aggregates of size from ~2 µm up to 242 µm with undefined shape was revealed; with the exception of empty "*kneaded 18 minutes at R.T. with 0.25 ml distilled water*" **γ-**CD where was seen a defined shape, i.e. prisms shape structure (Fig. $2c_2$). Similar observations on "the agglomeration of the free cyclodextrin", were revealed by Rakmai et al. (2017). It indicates the hydrogen bonding of the cyclodextrin molecules (empty) interact with each other in water producing the cluster of cyclodextrin. In addition, Shan et al. (2016) have demonstrated that CDs particle agglomeration might be induced also by moisture content.

The α-CD:OEO and γ-CD:OEO inclusion complexes morphology in the aqueous suspension was also revealed using TEM, and Fig. 3 shows clear lamella shapes with diameters of 0.1 µm - ~1 µm. In details, at 0.1 % (w/v) were detected single lamellas with diameters of 350 nm over a large number of grid holes (Fig. 3a), whereas in Figs. $3b_{1-3}$ were reported several representative TEM micrographs for 1 % (w/v), lamellas with diameters 170 - 519 nm. In addition, some of these lamellas fused together as indicated by the white arrow, indicating that the lamellas don't simply interact through their surfaces but are able to merge completely in aggregate. Thus, TEM measurements corroborated the results that were obtained from SEM, i.e. a well-defined lamella-shape structures of the inclusion complexes. In contrast, empty γ- CD (1 % w/v, aqueous suspension vortex 10 minutes at 2500 rpm, R.T) presented aggregates made up of a larger number of small spherical particles with diameters of about 5 nm - 325 nm (Figs. $3c_{1,2}$). These spherical particles seem to interact and form rodlike shape structure with diameters of about 406 nm - 1786 nm (inset of Figs. $3c_{3,4}$ diameter: 790.86 nm). Empty α-CD and α-CD:OEO inclusion complexes revealed similar morphologies (data not shown). These results support the hypothesis that the spherical particles are not indefinitely stable, thus tend to form a larger structure. These observations are in agreement with those revealed by several groups: Harada et al. (1990), (1992), (1993), and Ceccato et al. (1997) reported the formation of the so-called "molecular tube" a rodlike rigid molecule with an empty hydrophobic cavity that can behave as a host for ions or small organic molecules. Furthermore, Bonini et al. (2006) reported evidence of β-cyclodextrin self-aggregation in water; it was showed also that the concentration plays a critical key on their morphology: polydisperse spherical objects with diameters of about 100 nm were present at low concentration, whereas micrometer planar aggregates are predominated at higher concentrations.

Fig. 3

Finally, wide-angle X- ray diffraction (WAXD) studies were conducted to confirm the formation of CD:OEO inclusion complexes. According to Marques (2010) and references cited herein, X-ray powder diffraction is the most useful method for the detection of inclusion complexes formation, especially in the case of the guest in the form of liquid molecules (e.g. oils and volatiles), because the liquid guest molecules produce no diffraction patterns and any changes in the diffractogram reflects the formation of a new crystal lattice. Figs. 4a and 4b show the WAXD patterns of empty α-CD and γ- CD compared with their inclusion complexes. Empty α-CD and γ-CD differed from each other in their diffraction patterns. The WAXD pattern of empty α-CD and γ-CD revealed several diffraction peaks which are indicative of their crystalline nature, but, according to Rusa et al. (2002) for α-CD there are three salient peaks associated with its crystal structure occurring at 2θ = 12.1º, 14.5º, and 21.8º (Fig. 4a). In the diffract grams of both CD:OEO inclusion complexes, some of these characteristic diffraction peaks disappear.

In α-CD:OEO inclusion complex a new intense diffraction peak appeared at 2θ = 19.6º, which was not observed in empty α-CD. According to Rusa et al. (2002) the peak at 2θ ~20º in the WAXD of α-CD inclusion complexes is characteristic for the channel structure of α-CD when including long guest molecules and polymers in particular.

In γ-CD:OEO inclusion complex a new sharp diffraction pick at 2θ = 7.6º (Fig. 4b) was revealed; this pick was not observed in empty "as-received" γ-CD. According to Harada et al. (1996); Rusa et al. (2002) this pick has been suggested as an indicator for γ-CD inclusion complex channel structures. Hence, this behaviour could be attributed to an interaction between cyclodextrin and oregano essential oil showing the presence of a new solid phase.

Fig. 4

3.3. Morphology of the Electrospun CD:OEO inclusion complexes-containing PHBV Films

The SEM micrographs of the electrospun fibers of the neat PHBV and the fibers containing the γ-CD:OEO and α-CD:OEO inclusion complexes are shown in Fig. 5. The mean fiber diameters obtained from the SEM images are gathered in Table 3. The diameter of the electrospun fibers of neat PHBV were 0.89 ± 0.30 µm, being very similar to those reported in our previous research work (Melendez-Rodriguez et al., 2019). Figs. 5a, 5b, 5c, 5d, 5e show the PHBV fibers containing different concentrations of γ-CD:OEO inclusion complexes, that is, 10, 15, 20, 25, and 30 wt%, in which one can observe that the fiber diameters for all samples ranged between 0.87 – 0.91 µm. Up to 25 wt% γ-CD:OEO inclusion complexes, the electrospinning process yielded regular and continuous fibers of PHBV. In the case of the fibers containing 30 wt% γ-CD:OEO inclusion complexes, the fibrilar morphology was affected, losing the homogeneity and continuity due to the high concentration of CD. Figs. 5f, 5g, 5h, 5i, 5j shows the electrospun fibers of PHBV containing different concentrations of α-CD:OEO inclusion complexes, that is, 10, 15, 20, 25, and 30 wt%. The electrospun fibers containing 10 and 15 wt% α-CD:OEO showed mean diameters of approximately of 0.89 and 0.90 µm, respectively, being homogeneous and with smooth surfaces. The diameter for the fibers containing 20 wt% α-CD:OEO inclusion complexes increased, with a mean value of 1.03 ± 0.25 µm, and it also presented beaded regions due to potential CD agglomerations. The fibers with 25 and 30 wt% α-CD:OEO inclusion complexes, shown respectively in Figs. 5i, 5j, presented diameters of 1.17 and 1.22 µm. This slight increase in the fiber diameters can be related to the relatively high amount of CDs that aggregated during electrospinning and resulted in destabilization of the electrified jet. The present results agree with the reports of (Topuz & Uyar, 2019), concluding that at low hydroxypropyl-β-CD/Laponite the fibers do not present any significant change in diameter and shape while at high concentrations the nanocomposite nanofibers from a non-polymeric system diameter decreases and also generates aggregates. Furthermore, changes in the solution properties such as viscosity or conductivity may cause variations in the electrospun morphologies. For instance, Aytac, Ipek, Durgun, Tekinay, & Uyar (2017) determined that the diameters of nanofibers containing methylated-β-CD/linalool were lower than those of hydroxypropyl-β-CD/linalool due to the lower viscosity and higher conductivity of the aqueous solution. Therefore, the most optimal fibrillary morphologies were attained for PHBV containing 25 wt% γ-CD:OEO inclusion complexes and 15 wt% α-CD:OEO inclusion complexes.

Fig. 5

Table 3

The electrospun fibers mats were subjected to annealing in order to obtain a continuous film (Figueroa-Lopez et al., 2019; Melendez-Rodriguez et al., 2019). The surface and cross-section areas of the PHBV films containing $\boldsymbol{\gamma}$-CD:OEO inclusion complexes and $\boldsymbol{\alpha}$-CD:OEO inclusion complexes were observed by SEM images. As shown in Fig. 6, the surface of the electrospun PHBV films containing 10, 15, 20, and 25 wt% $\boldsymbol{\gamma}$-CD:OEO inclusion complexes were homogeneous and continuous with a mean thickness of approximately 61 ± 1.1, 63 ± 0.98, 70 ± 0.94, and 72 ± 0.72 µm, respectively (*see* Table 3). This is in agreement with the electrospun fiber morphologies described above (*see* Fig. 5) that showed proper fiber formation until 25 wt%. Moreover, the film containing 30 wt% showed a surface with some cracks due to the high concentration of $\boldsymbol{\gamma}$-CD:OEO inclusion complexes that difficulted the formation of a continuous film with higher thickness (~ 77 ± 0.68 µm). The film thicknesses also increased with the concentration of $\boldsymbol{\gamma}$-CD:OEO inclusion complexes. Based on these results, the best concentration to attain uniform and homogenous films of PHBV was 25 wt% $\boldsymbol{\gamma}$-CD:OEO inclusion complexes.

Fig. 6

Fig. 7 showed the surface and cross-section of the films containing α-CD:OEO inclusion complexes. The thicknesses of the films containing 10 and 15 wt% α-CD:OEO inclusion complexes were 73 ± 0.99 and 75 ± 0.77 µm, respectively. These films also showed a homogeneous surface. When the concentrations of α-CD:OEO inclusion complexes increased, the thicknesses were also higher, reaching values of 81 ± 0.91, 83 ± 0.86, and 85 ± 0.69 µm for 20, 25, and 30 wt% α-CD:OEO, respectively (*see* Table 3). Increasing the concentration from 20 wt% also affected the surface and generated cracks with different sizes. This phenomenon has been ascribed to the weak interfacial bond between the CDs and the biopolyester matrix (Ashori, Jonoobi, Ayrilmis, Shahreki, & Fashapoyeh, 2019). Melendez-Rodriguez et al. (2019) also found that at high concentrations of silica nanoparticles with eugenol, that is, 15 and 20 wt%, the electrospun films showed greater porosity and also some plastic deformation, which was attributed to a plasticization generated by the released oil and a possible migration during the annealing process. In this case, the best concentration to get uniform and homogenous films was 15 wt% α-CD:OEO inclusion complexes.

Fig. 7

3.1. Visual Aspect of the Electrospun CD:OEO-containing PHBV Films

The visual aspect of the electrospun PHBV films containing different concentrations of γ-CD:OEO and α-CD:OEO was observed to ascertain their contact transparency. In Fig. 8 it can be observed that the contact transparency was high and though some differences among the samples were seen. The neat PHBV film had a transparency value of 4.78 ± 0.08 and opacity of 0.037 ± 0.001. When 10 wt% γ-CD:OEO was incorporated, slight changes were observed with respect to the neat PHBV´s transparency whereas opacity values without significant differences were obtained. The transparency value and opacity of the films containing 15, 20, and 25 wt% γ-CD:OEO increased significantly respect to neat PHBV and 10 wt%. When was incorporate 30 wt% γ-CD:OEO the transparency and opacity values were higher respect to the others samples (9.23 ± 0.59 and 0.065 ± 0.004, respectively). Also, the films containing α-CD:OEO presented high changes in the transparency and opacity respect to the γ-CD:OEO. In particular, for the film sample containing 10 wt% α-CD:OEO, a transparency value of 6.36 ± 0.63 and opacity of 0.047 ± 0.005 was obtained. For the 15 and 20 wt% α-CD:OEO-containing films the values were similar while those based on 25 and 30 wt% α-CD:OEO presented the highest values. For both inclusion complexes, the increment of the concentration caused a light scattering that produced lower transparency and higher opacity. This phenomenon can be important in the design of food packaging materials due to some food products are sensible to the ultraviolet-visible (UV-Vis) light, which can trigger different enzymatic and oxidative reactions (Figueroa-Lopez et al., 2018).

Fig. 8

3.2. Thermal Stability of the Electrospun CD:OEO-containing PHBV Films

The TGA curves for the neat PHBV, γ-CD, α-CD, inclusion complexes of γ-CD:OEO and α-CD:OEO, and the PHBV films containing the inclusion complexes are shown in Fig. 9. The values of mass loss at 5% ($T_{5\%}$), mass at 160 ºC (%), which corresponds to annealing temperature of the films (*see* section 2.4.2), degradation temperature (T_{deg}), weight loss at T_{deg} (%), and residual mass (%) at 700 °C are gathered in Table 4. In our previous study, the TGA curve for the neat OEO showed a low thermal stability, presented a mass loss at 160 ºC around of 40.3 %, with its T_{deg} value was 178.4 °C and mass loss was 74.16% at T_{deg}, corresponding to the volatilization and/or degradation of principal volatile compounds, such as carvacrol, thymol, and pinene (Figueroa-Lopez et al., 2019). This value is similar to the value of T_{deg} of 168 ºC reported by (Guimarães et al., 2015). The mass loss at 160 ºC for the empty CDs were 8.86 % (γ-CD) and 9.42 % (α-CD), while the T_{deg} values were 323.12 ºC with a mass loss of 83.01 % for γ-CD and 326.43 ºC with a mass loss of 86.29 % for α-CD. As other authors have indicated, the thermal degradation of powdered molecules can be affected by different factors such as chemical structure, crystallinity, crystal size, and morphology (Campos et al., 2018; Kohata, Jyodoi, & Ohyoshi, 1993). Thus, the thermal stability of CDs depends on the size of the crystal, showing greater thermal stability the larger crystals (Giordano, Novak, & Moyano, 2001; Nakanishi et al., 1997). When the essential oil was encapsulated into CDs, the inclusion complexes enhanced the thermal stability due to the interactions between the guest molecule and the cavity of the cyclodextrins achieving a protection of the volatiles compounds (Kayaci & Uyar, 2012). The mass loss for γ-CD:OEO inclusion complexes at 160 ºC was nearly 16.9%, having a T_{deg} of 326.28 ºC with a mass loss of 86.11 % at T_{deg}. In the case of α-CD:OEO inclusion complexes, the mass loss at 160 ºC was 9.69% and T_{deg} was 330.50 ºC with a mass loss at T_{deg} of approximately 85.70%. The inclusion complexes showed two mass losses, one below 100 °C corresponding to the loss of water from the cavity and another above 280 °C, which is attributed to the main thermal degradation of CDs (Aytac et al., 2017). Shin, Kathuria, & Lee (2019) reported similar results for triacetyl (TA) encapsulated in β-CD, obtaining a T_{deg} of 293.99 °C for β-CD and for the inclusion complex of TA-β-CD its T_{deg} was 340.62 ºC. The thermal degradation of the PHBV films containing inclusion complexes increased slightly the value of T_{deg} respect to the neat PHBV. The mass loss values at 160 ºC for all films containing CDs and the inclusion complexes were similar, showing values between 1.21 – 1.71%. The slight differences can be ascribed to the size and load capacity of the two tested CDs. The value of T_{deg} for the PHBV with 25 wt% γ-CD:OEO was 322.52 ºC with a mass loss of 96.12 %, while T_{deg} for the PHBV with 25 wt% γ-CD without OEO was slightly lower (320.11 ºC). Furthermore, the PHBV film containing 15 wt% α-CD:OEO showed a T_{deg} around 313.70 ºC with a mass loss of 96.98 % and the films with 15 wt% α-CD without OEO presented a T_{deg} of 309.27 ºC and mass loss around 96.28 %. Then, the thermal stability of OEO was improved in the electrospun PHBV films. In this regard, (Yildiz, Celebioglu, Kilic, Durgun, & Uyar, 2018) reported an improvement of the thermal stability of CD:menthol inclusion complex in aqueous solutions nanofibers. Other studies have also suggested that the addition of substances such as powder, nanoparticles, EOs into electrospun biopolymer films increased the maximum decomposition temperature (Melendez-Rodriguez et al., 2019; Quiles-Carrillo, Montanes, Lagaron, Balart, & Torres-Giner, 2019b; Zainuddin, Kamrul Hasan, Loeven, & Hosur, 2019).

Fig. 9

Table 4

3.3. Mechanical Properties of the Electrospun CD:OEO-containing PHBV Films

The mechanical properties of the electrospun PHBV films containing the inclusion complexes are shown in Table 5. The neat PHBV film presented a E value of 1252 MPa, a σ_b value of 18.1 MPa, and a $\square_b$ value of 2.4%, being very similar values than those reported in our previous work (Melendez-Rodriguez et al., 2019). The elastic modulus increased when CDs were included in the PHBV matrix. The E value for the PHBV film with 25% wt γ-CD was 1692 MPa and for the PHBV film with 15% wt α-CD, the E value was 1594 MPa. Likewise, the E values were higher in the PHBV films containing CDs with OEO compared with the films with CDs without OEO, showing a E value of 1472 MPa for the PHBV with 25% wt γ-CD:OEO and an E value of 1698 MPa for the PHBV with 25% wt α-CD:OEO. These significant increases of elasticity of PHBV films were induced by the presence of powder particles, that is, CDs, which potentially generated low interfacial interactions between the hydrophilic compounds of γ-CD and α-CD and the hydrophobic PHBV matrix and OEO, producing a reduction in ductility and consequently an increment in mechanical resistance (Zainuddin et al., 2019). Indeed, the values of σ_b decreased in the PHBV containing CDs, with values between 9.04 MPa and 9.83 MPa, while the $\square_b$ values of PHBV films also decreased from 2.4% to 0.78 % due to presence of CDs and OEO. As reported by (Shin et al., 2019), the addition of β-CD containing allyl isothiocyanate (AITC) reduced the tensile strength and elongation by 84% and 96%, respectively, of LDPE films obtained by extrusion. In another work, (Melendez-Rodriguez et al., 2019) reported an improvement of the elastic modulus and tensile strength of electrospun PHBV films when mesoporous silica nanoparticles containing eugenol were incorporated. The PHBV films here-prepared with the inclusion complexes are slightly less deformable and therefore have greater elasticity than films produced using other commercial biopolymers, which facilitates the development of materials for the design of packaging to protect food (Quiles-Carrillo et al., 2019b).

Table 5

3.4. Antimicrobial activity of the Electrospun CD:OEO-containing PHBV Films

Table 6 showed the MIC and MBC values of γ-CD:OEO, and α-CD:OEO against *S. aureus* and *E. coli*. In our previous studies it was reported that the MIC and MBC for pure OEO against *S. aureus* was 0.312 µL/mL and for *E. coli* was 0.625 µL/mL (Figueroa-Lopez et al., 2019). Results showed that the encapsulation of OEO in CDs increased the antibacterial activity. The MIC and MBC values of γ-CD:OEO against *S. aureus* was 0.039 µg/mL and against *E. coli* was 0.078 µg/mL. In the case of α-CD:OEO, the MIC ad MBC values were 0.078 µg/mL, against *S. aureus*, and 0.156 µg/mL, against *E. coli,* so that these values agree with that reported by (Liang, Yuan, Vriesekoop, & Lv, 2012) for α-CD/carvacrol (MIC = 0.125 µg/mL). The higher antibacterial activity of γ-CD:OEO inclusion complexes can be attributed to its higher cavity size, encapsulation efficiency, and loading capacity compared with α-CD:OEO inclusion complexes, as reported above in Table 2. For both inclusion complexes, *S. aureus* was more sensitive than *E. coli*. In this regard, inclusion complexes have been reported to elevate the aqueous solubility of encapsulated hosts resulting in improved antimicrobial efficiency of EOs and their components at lower concentration (Das et al., 2019). (M. Zhang et al., 2018) evaluated the antimicrobial activity of γ-CD/alamethicin complex against *L. monocytogenes*, showing that the use of CD increased the solubility of alamethicin in aqueous medium thereby allowing more alamethicin to interact with the cell membranes resulting in higher antimicrobial activity.

Table 6

Figs. 10a and 10b show the antibacterial activity results of the PHBV films containing 25 wt% γ-CD:OEO and 15 wt% α-CD:OE in an open and closed system for up to 15 days. The films used as control (samples without the inclusion complexes) presented an *E. coli* and *S. aureus* growth in the range between 4.16 x 10^6 and 6.05 x 10^6 CFU/mL. As shown in Fig. 10a, the reduction versus *S. aureus* and *E. coli* for the films containing 25 wt% γ-CD:OEO was strong (R ≥ 3), reaching a reduction for up to 3.63 and 3.28 Log_{10} (CFU/mL), respectively, after 15 days of evaluation. The PHBV films containing 15 wt% α-CD:OEO at day 1 presented a significant inhibition (R ≥ 1 and <3) and at days 3, 8, and 15 the inhibition was strong showing a reduction of up to 3.15 Log_{10} (CFU/mL) against *S. aureus*. The inhibition achieved for *E. coli* was significant, obtaining a reduction of 2.64 Log_{10} (CFU/mL) at day 15. These results correlate well with the antimicrobial properties included in Table 6 and Fig. 10 that show that the antibacterial activity of the γ-CD:OEO inclusion complexes was higher than the α-CD:OEO inclusion complexes.

The reduction of the *S. aureus* and *E. coli* using PHBV films containing 25 wt% γ-CD:OEO inclusion complexes and 15 wt% α-CD:OEO inclusion complexes in a closed system for up to 15 days of analysis are showed in Fig. 10b. All values in the closed system showed slightly higher values of reduction compared with the open system due to the release of the volatile compounds that were accumulated in the headspace. The film containing 25 wt% γ-CD:OEO inclusion complexes presented a strong activity against both bacteria during the 15 days of the study (R ≥ 3). The antimicrobial activity for γ-CD:OEO inclusion complexes was higher than α-CD:OEO inclusion complexes, which is in accordance to the characteristics of this type of CD, that are, a higher solubility and a bigger pore size (-γ) (Szejtli, 1998). Moreover, this is produced by the CD inclusion complexes mechanism that increases the solubility and therefore provides an efficient release of the hydrophobic agent in bacterial medium (Liang et al., 2012). Likewise, (Celebioglu, Umu, Tekinay, & Uyar, 2014) observed that films containing triclosan/HPβCD and triclosan/HPγCD inclusion complexes showed better antibacterial activity against both bacteria compared to the film with uncomplexed pure triclosan. Furthermore, the inhibition of *S. aureus* was slightly higher compared to *E. coli* due to the cellular wall differences between Gram negative (G-) and Gram positive (G+) bacteria (Rakmai, Cheirsilp, Mejuto, Torrado-Agrasar, & Simal-Gándara, 2017).

Fig. 10

3.4.1. Antioxidant Activity of the Electrospun CD:OEO-containing PHBV Films

The inhibition percentage (%) of DPPH and concentration (eq. trolox/g sample) of DPPH for the pure OEO, γ-CD:OEO inclusion complexes, α-CD:OEO inclusion complexes, and the electrospun PHBV films containing γ-CD:OEO and α-CD:OEO are shown in Fig. 11 and Table 7. These systems were also evaluated in an open and closed system for 15 days. Neat OEO presented a high percentage of inhibition (91.96%) attributed to its main active compounds (*i.e.,* carvacrol, thymol, p-cymene, γ-terpinene) (Figueroa-Lopez et al., 2019). The DPPH inhibition for γ-CD:OEO inclusion complexes was 82.51 % and for α-CD:OEO inclusion complexes it was 76.32 %. Therefore, OEO decreased the percentage of inhibition when it was encapsulated in CDs, which can be related to the encapsulation efficiency and loading capacity of the inclusion complexes reported above (*see* Table 2). The higher antioxidant activity attained with γ-CD:OEO inclusion complexes can be related to its greater encapsulation efficiency when compared with α-CD:OEO inclusion complexes. As indicated by Lu, Cheng, Hu, Zhang, & Zou (2009) the antioxidant activity of resveratrol in free form showed little difference with that of resveratrol in complex form at the same concentration.

The antioxidant activity of biodegradable films is generally proportional to the amount of antioxidant additives added whereas the thermal process to obtain the films cab also highly affect bioactivity since most bioactive compounds are sensitive to temperatures above 80 °C (Jouki, Yazdi, Mortazavi, & Koocheki, 2014). The electrospun films containing OEO, that is, PHBV with 10 wt% OEO, showed a low inhibition of DPPH (24.54%) with respect to the films containing the inclusion complexes, which were 53.16% for PHBV with 25 wt% γ-CD:OEO inclusion complexes and 45.34% for PHBV with 15 wt% α-CD:OEO inclusion complexes, at day 1 of evaluation. From day 3, all the PHBV films started to show lower antioxidant activity. In the closed system, the films presented a slightly higher DPPH inhibition than the films of the open system due to the release of OEO volatile compounds to the packaging headspace. For the last day of evaluation, that is, day 15, the PHBV with 10 wt% OEO films showed an inhibition of DPPH in the open and closed system of 14.90–15.24 % (15.75 - 16.47 μg eq trolox/g sample), respectively. The PHBV film containing 15 wt% α-CD:OEO inclusion compelxes presented an inhibition of 36.11–37.24 % (38.42 - 39.26 μg eq trolox/g sample) while the PHBV film with 25 wt% γ-CD:OEO inclusion complexes presented the highest antioxidant activity with a DPPH inhibition of 45.26–47.02 % (48.17 - 49.95 μg eq trolox/g sample). These results demonstrate that the here-prepared inclusion complexes can successfully protect the volatile compounds responsible for the active properties of OEO, a thermolabile substance, in a similar way that observed above in the antimicrobial test. These results also agree with the research work of (Aytac et al., 2017) where the antioxidant activity of electrospun fibers of PLA containing $\beta-\mathrm{CD}$:gallic acid was slightly superior to the fibers of PLA containing neat gallic acid, being this effect attributed to the solubility of gallic acid in alcohols and the position of gallic acid in the cavity of β-CD.

Likewise, Kaolaor, Phunpee, Ruktanonchai, & Suwantong (2019) determined a high antioxidant activity of β − CD:curcumin in poly(vinyl alcohol) (PVOH) blend films, which was attributed to the complexity of curcumin in the cavity of β-CD. In conclusion, the electrospun films of PHBV with 25 wt% γ-CD:OEO inclusion complexes managed to maintain a high antioxidant activity for a longer period, which indicates that this material can be used in the design of active packaging that helps to maintain the physical, chemical, and microbiological characteristics of the food products (Robertson, 2005).

Fig. 11

Table 7

4. Conclusions

The KM and FDM were used to prepare inclusion complexes between α- and γ-CD (host) and oregano essential oil (guest). Both methods presented high encapsulation efficiencies, with KM complexes having higher encapsulation efficiencies than FDM based ICs, that can be justified by the shear rate applied. In addition, besides of shear rate, other factors, such as weight ratio host-guest (80:20 w/w and 85:15 w/w) and types of wall materials (α- and γ-CD); solvent quantity (KM: 0.25 ml and FDM: 2.5 ml); and mixing time (KM:18 minutes towards FDM □ 48 h for the formation of inclusion complex) might affects the properties of the obtained complexes such as encapsulation efficiency. KM revealed to be the most efficient method for encapsulation of oregano essential oil in CD cavity, and moreover it added value also in terms of rapidity (KM: 18 minutes towards FDM □ 48 h for the formation of inclusion complex), and the desired characteristics of the final product (γ-CD: oregano essential oil (80:20 w/w) – EE, % of 98.5 ± 0.7 and LC, % of 19.6 ± 0.1).

The inclusion complexes presented a high antimicrobial and antioxidant activity, which allowed their addition to the PHBV fibers for film formation. The best concentration of inclusion complexes for homogeneous and continuous film formation were 25 wt% γ-CD:OEO inclusion complexes and 15 wt% α-CD:OEO inclusion complexes. The addition of the inclusion complexes in the PHBV matrix improved the mechanical and thermal properties. Likewise, the antimicrobial and antioxidant activity of the films were maintained by 15 days, due to the encapsulation system, that protects bioactive compounds. The improved properties of PHBV films allow their application in the design of biodegradable active packaging systems to contain food and extend their shelf life.

Acknowledgments: The authors would like to thank the Unidad Asociada IATA-UJI "Plastics Technology" and to the Spanish Ministry of Economy and Competitiveness (MINECO) project RTI2018-097249-B-C21 and the H2020 EU project YPACK (reference number 773872) for funding. Kelly J. Figueroa-Lopez is recipient of a Grisolia (Ref. 0001426013N810001A201) research contract of the Valencian Government.

References

Ashori, A., Jonoobi, M., Ayrilmis, N., Shahreki, A., & Fashapoyeh, M. A. (2019). Preparation and characterization of polyhydroxybutyrate-co-valerate (PHBV) as green composites using nano reinforcements. *International Journal of Biological Macromolecules, 136*, 1119-1124. doi:https://doi.org/10.1016/j.ijbiomac.2019.06.181

Aytac, Z., Ipek, S., Durgun, E., Tekinay, T., & Uyar, T. (2017). Antibacterial electrospun zein nanofibrous web encapsulating thymol/cyclodextrin-inclusion complex for food packaging. *Food Chemistry, 233*, 117-124. doi:https://doi.org/10.1016/j.foodchem.2017.04.095

Bakhtiary, F., Sayevand, H. R., Khaneghah, A. M., Haslberger, A. G., & Hosseini, H. (2018). Antibacterial efficacy of essential oils and sodium nitrite in vacuum processed beef fillet. *Applied Food Biotechnology, 5*(1), 1-10. doi:10.22037/afb.v5i1.17118

Bakkali, F., Averbeck, S., Averbeck, D., & Idaomar, M. (2008). Biological effects of essential oils – A review. *Food and Chemical Toxicology, 46*(2), 446-475. doi:https://doi.org/10.1016/j.fct.2007.09.106

Beirão-da-Costa, S., Duarte, C., Bourbon, A. I., Pinheiro, A. C., Januário, M. I. N., Vicente, A. A., . . . Delgadillo, I. (2013). Inulin potential for encapsulation and controlled delivery of Oregano essential oil. *Food Hydrocolloids, 33*(2), 199-206. doi:https://doi.org/10.1016/j.foodhyd.2013.03.009

Bilia, A. R., Guccione, C., Isacchi, B., Righeschi, C., Firenzuoli, F., & Bergonzi, M. C. (2014). Essential oils loaded in nanosystems: a developing strategy for a successful therapeutic approach. *Evidence-based complementary and alternative medicine : eCAM, 2014*, 651593-651593. doi:10.1155/2014/651593

Busolo, M. A., & Lagaron, J. M. (2015). Antioxidant polyethylene films based on a resveratrol containing Clay of Interest in Food Packaging Applications. *Food Packaging and Shelf Life, 6*, 30-41. doi:10.1016/j.fpsl.2015.08.004

Campos, E. V. R., Proença, P. L. F., Oliveira, J. L., Melville, C. C., Della Vechia, J. F., de Andrade, D. J., & Fraceto, L. F. (2018). Chitosan nanoparticles functionalized with β-cyclodextrin: a promising carrier for botanical pesticides. *Scientific Reports, 8*(1), 2067. doi:10.1038/s41598-018-20602-y

Ceccato, M., Lo Nostro, P., Rossi, C., Bonechi, C., Donati, A., & Baglioni, P. (1997). Molecular Dynamics of Novel α-Cyclodextrin Adducts Studied by 13C-NMR Relaxation. *The Journal of Physical Chemistry B, 101*(26), 5094-5099. doi:10.1021/jp9638447

Celebioglu, A., Umu, O. C. O., Tekinay, T., & Uyar, T. (2014). Antibacterial electrospun nanofibers from triclosan/cyclodextrin inclusion complexes. *Colloids and Surfaces B: Biointerfaces, 116*, 612-619. doi:https://doi.org/10.1016/j.colsurfb.2013.10.029

Crini, G. (2014). Review: A History of Cyclodextrins. *Chemical Reviews, 114*(21), 10940-10975. doi:10.1021/cr500081p

Cherpinski, A., Torres-Giner, S., Cabedo, L., & Lagaron, J. M. (2017). Post-processing optimization of electrospun submicron poly(3-hydroxybutyrate) fibers to obtain continuous films of interest in food packaging applications. *Food Additives and Contaminants - Part A Chemistry, Analysis, Control, Exposure and Risk Assessment, 34*(10), 1817-1830. doi:10.1080/19440049.2017.1355115

Das, S., Gazdag, Z., Szente, L., Meggyes, M., Horváth, G., Lemli, B., . . . Kőszegi, T. (2019). Antioxidant and antimicrobial properties of randomly methylated β cyclodextrin – captured essential oils. *Food Chemistry, 278*, 305-313. doi:https://doi.org/10.1016/j.foodchem.2018.11.047

Das, S., & Subuddhi, U. (2015). Studies on the complexation of diclofenac sodium with β–cyclodextrin: Influence of method of preparation. *Journal of Molecular Structure, 1099*, 482-489. doi:https://doi.org/10.1016/j.molstruc.2015.07.001

De Vincenzi, M., Stammati, A., De Vincenzi, A., & Silano, M. (2004). Constituents of aromatic plants: carvacrol. *Fitoterapia, 75*(7), 801-804. doi:https://doi.org/10.1016/j.fitote.2004.05.002

Del Valle, E. M. M. (2004). Cyclodextrins and their uses: a review. *Process Biochemistry, 39*(9), 1033-1046. doi:https://doi.org/10.1016/S0032-9592(03)00258-9

Dietrich, K., Dumont, M.-J., Del Rio, L. F., & Orsat, V. (2019). Sustainable PHA production in integrated lignocellulose biorefineries. *New Biotechnology, 49*, 161-168. doi:https://doi.org/10.1016/j.nbt.2018.11.004

EU 872/2012; Annex I of Regulation 1334/2008; EU 2018/1259; http://data.europa.eu/eli/reg/2018/1259/oj

Figueroa-Lopez, K., Andrade-Mahecha, M., & Torres-Vargas, O. (2018). Development of antimicrobial biocomposite films to preserve the quality of bread. *Molecules, 23*(1), 212.

Figueroa-Lopez, K. J., Castro-Mayorga , J. L., Andrade-Mahecha, M. M., Cabedo, L., & Lagaron, J. M. (2018). Antibacterial and Barrier Properties of Gelatin Coated by Electrospun Polycaprolactone Ultrathin Fibers Containing Black Pepper Oleoresin of Interest in Active Food Biopackaging Applications. *Nanomaterials, 8*(4), 1-13.

Figueroa-Lopez, K. J., Vicente, A. A., Reis, M. A. M., Torres-Giner, S., & Lagaron, J. M. (2019). Antimicrobial and Antioxidant Performance of Various Essential Oils and Natural Extracts and Their Incorporation into Biowaste Derived Poly(3-hydroxybutyrate-co-3-hydroxyvalerate) Layers Made from Electrospun Ultrathin Fibers. *Nanomaterials, 9*(2). doi:10.3390/nano9020144

Gao, N., Yang, J., Wu, Y., Yue, J., Cao, G., Zhang, A., . . . Feng, Z. (2019). β-Cyclodextrin functionalized coaxially electrospun poly(vinylidene fluoride) @ polystyrene membranes with higher mechanical performance for efficient removal of phenolphthalein. *Reactive and Functional Polymers, 141*, 100-111. doi:https://doi.org/10.1016/j.reactfunctpolym.2019.05.001

Gaur, S., Lopez, E. C., Ojha, A., & Andrade, J. E. (2018). Functionalization of Lipid-Based Nutrient Supplement with β-Cyclodextrin Inclusions of Oregano Essential Oil. *Journal of Food Science, 83*(6), 1748-1756. doi:10.1111/1750-3841.14178

Giordano, F., Novak, C., & Moyano, J. R. (2001). Thermal analysis of cyclodextrins and their inclusion compounds. *Thermochimica Acta, 380*(2), 123-151. doi:https://doi.org/10.1016/S0040-6031(01)00665-7

Guimarães, A. G., Oliveira, M. A., Alves, R. d. S., Menezes, P. d. P., Serafini, M. R., de Souza Araújo, A. A., . . . Quintans Júnior, L. J. (2015). Encapsulation of carvacrol, a monoterpene present in the essential oil of oregano, with β-cyclodextrin, improves the pharmacological response on cancer pain experimental protocols. *Chemico-Biological Interactions, 227*, 69-76. doi:https://doi.org/10.1016/j.cbi.2014.12.020

Haloci, E., Toska, V., Shkreli, R., Goci, E., Vertuani, S., & Manfredini, S. (2014). Encapsulation of Satureja montana essential oil in β-cyclodextrin. *Journal of Inclusion Phenomena and Macrocyclic Chemistry, 80*(1), 147-153. doi:10.1007/s10847-014-0437-z

Harada, A., & Kamachi, M. (1990). Complex formation between poly(ethylene glycol) and α-cyclodextrin. *Macromolecules, 23*(10), 2821-2823. doi:10.1021/ma00212a039

Harada, A., Li, J., & Kamachi, M. (1992). The molecular necklace: a rotaxane containing many threaded α-cyclodextrins. *Nature, 356*(6367), 325-327. doi:10.1038/356325a0

Harada, A., Li, J., & Kamachi, M. (1993). Synthesis of a tubular polymer from threaded cyclodextrins. *Nature, 364*(6437), 516-518. doi:10.1038/364516a0

Harada, A., Suzuki, S., Okada, M., & Kamachi, M. (1996). Preparation and Characterization of Inclusion Complexes of Polyisobutylene with Cyclodextrins. *Macromolecules, 29*(17), 5611-5614. doi:10.1021/ma960428b

Hedges, A. R. (1998). Industrial Applications of Cyclodextrins. *Chemical Reviews, 98*(5), 2035-2044. doi:10.1021/cr970014w

Hill, L. E., Gomes, C., & Taylor, T. M. (2013). Characterization of beta-cyclodextrin inclusion complexes containing essential oils (trans-cinnamaldehyde, eugenol, cinnamon bark, and clove bud extracts) for antimicrobial delivery applications. *LWT - Food Science and Technology, 51*(1), 86-93. doi:https://doi.org/10.1016/j.lwt.2012.11.011

Hosseini, S. F., Zandi, M., Rezaei, M., & Farahmandghavi, F. (2013). Two-step method for encapsulation of oregano essential oil in chitosan nanoparticles: Preparation, characterization and in vitro release study. *Carbohydrate Polymers, 95*(1), 50-56. doi:https://doi.org/10.1016/j.carbpol.2013.02.031

Jouki, M., Yazdi, F. T., Mortazavi, S. A., & Koocheki, A. (2014). Quince seed mucilage films incorporated with oregano essential oil: Physical, thermal, barrier, antioxidant and antibacterial properties. *Food Hydrocolloids, 36*, 9-19. doi:https://doi.org/10.1016/j.foodhyd.2013.08.030

Ju, J., Chen, X., Xie, Y., Yu, H., Guo, Y., Cheng, Y., . . . Yao, W. (2019). Application of essential oil as a sustained release preparation in food packaging. *Trends in Food Science & Technology, 92*, 22-32. doi:https://doi.org/10.1016/j.tifs.2019.08.005

Kaolaor, A., Phunpee, S., Ruktanonchai, U. R., & Suwantong, O. (2019). Effects of β-cyclodextrin complexation of curcumin and quaternization of chitosan on the properties of the blend films for use as wound dressings. *Journal of Polymer Research, 26*(2), 43. doi:10.1007/s10965-019-1703-y

Kayaci, F., & Uyar, T. (2012). Encapsulation of vanillin/cyclodextrin inclusion complex in electrospun polyvinyl alcohol (PVA) nanowebs: Prolonged shelf-life and high temperature stability of vanillin. *Food Chemistry, 133*(3), 641-649. doi:https://doi.org/10.1016/j.foodchem.2012.01.040

Kohata, S., Jyodoi, K., Ohyoshi, A. (1993). Thermal decomposition of cyclodextrins (α-, β-, γ-, and modified β-CyD) and of metal—(β-CyD) complexes in the solid phase. *Thermochimica Acta, 217,* 187-198. https://doi.org/10.1016/0040-6031(93)85107-K

Li, D., & Xia, Y. (2004). Electrospinning of Nanofibers: Reinventing the Wheel? *Advanced Materials, 16*(14), 1151-1170. doi:10.1002/adma.200400719

Liang, H., Yuan, Q., Vriesekoop, F., & Lv, F. (2012). Effects of cyclodextrins on the antimicrobial activity of plant-derived essential oil compounds. *Food Chemistry, 135*(3), 1020-1027. doi:https://doi.org/10.1016/j.foodchem.2012.05.054

Loftsson, T., & Brewster, M. E. (1996). Pharmaceutical Applications of Cyclodextrins. 1. Drug Solubilization and Stabilization. *Journal of Pharmaceutical Sciences, 85*(10), 1017-1025. doi:https://doi.org/10.1021/js950534b

Lu, Z., Cheng, B., Hu, Y., Zhang, Y., & Zou, G. (2009). Complexation of resveratrol with cyclodextrins: Solubility and antioxidant activity. *Food Chemistry, 113*(1), 17-20. doi:https://doi.org/10.1016/j.foodchem.2008.04.042

Marques, H. M. C. (2010). A review on cyclodextrin encapsulation of essential oils and volatiles. *Flavour and Fragrance Journal, 25*(5), 313-326. doi:10.1002/ffj.2019

Melendez-Rodriguez, B., Figueroa-Lopez, J. K., Bernardos, A., Martínez-Máñez, R., Cabedo, L., Torres-Giner, S., & M. Lagaron, J. (2019). Electrospun Antimicrobial Films of Poly(3-hydroxybutyrate-co-3-hydroxyvalerate) Containing Eugenol Essential Oil Encapsulated in Mesoporous Silica Nanoparticles. *Nanomaterials, 9*(2). doi:10.3390/nano9020227

Nakanishi, K., Masukawa, T., Nadai, T., Yoshii, K., Okada, S., & Miyajima, K. (1997). Sustained Release of Flufenamic Acid from a Drug-Triacetyl-β-Cyclodextrin Complex. *Biological & Pharmaceutical Bulletin, 20*(1), 66-70. doi:10.1248/bpb.20.66

Owen, L., & Laird, K. (2018). Synchronous application of antibiotics and essential oils: dual mechanisms of action as a potential solution to antibiotic resistance. *Critical Reviews in Microbiology, 44*(4), 414-435. doi:10.1080/1040841X.2018.1423616

Ozdemir, N., Pola, C. C., Teixeira, B. N., Hill, L. E., Bayrak, A., & Gomes, C. L. (2018). Preparation of black pepper oleoresin inclusion complexes based on beta-cyclodextrin for antioxidant and antimicrobial delivery applications using kneading and freeze drying methods: A comparative study. *LWT - Food Science and Technology, 91*, 439-445. doi:10.1016/j.lwt.2018.01.046

Petrovi, G. M., Stojanovi, G. S., & Radulovi, N. S. (2010). Encapsulation of cinnamon oil in β-cyclodextrin. *Journal of medicinal plant research, 4*(14), 1382-1390.

Ponce Cevallos, P. A., Buera, M. P., & Elizalde, B. E. (2010). Encapsulation of cinnamon and thyme essential oils components (cinnamaldehyde and thymol) in β-cyclodextrin: Effect of interactions with water on complex stability. *Journal of Food Engineering, 99*(1), 70-75. doi:https://doi.org/10.1016/j.jfoodeng.2010.01.039

Prakash, B., Kedia, A., Mishra, P. K., & Dubey, N. K. (2015). Plant essential oils as food preservatives to control moulds, mycotoxin contamination and oxidative deterioration of agri-food commodities –

Potentials and challenges. *Food Control, 47*, 381-391. doi:https://doi.org/10.1016/j.foodcont.2014.07.023

Prakash, B., Singh, P., Kedia, A., & Dubey, N. K. (2012). Assessment of some essential oils as food preservatives based on antifungal, antiaflatoxin, antioxidant activities and in vivo efficacy in food system. *Food Research International, 49*(1), 201-208. doi:https://doi.org/10.1016/j.foodres.2012.08.020

Quiles-Carrillo, L., Montanes, N., Lagaron, J. M., Balart, R., & Torres-Giner, S. (2019a). Bioactive multilayer polylactide films with controlled release capacity of gallic acid accomplished by incorporating electrospun nanostructured coatings and interlayers. *Applied Sciences (Switzerland), 9*(3). doi:10.3390/app9030533

Quiles-Carrillo, L., Montanes, N., Lagaron, J. M., Balart, R., & Torres-Giner, S. (2019b). In Situ Compatibilization of Biopolymer Ternary Blends by Reactive Extrusion with Low-Functionality Epoxy-Based Styrene–Acrylic Oligomer. *Journal of Polymers and the Environment, 27*(1), 84-96. doi:10.1007/s10924-018-1324-2

Rakmai, J., Cheirsilp, B., Mejuto, J. C., Torrado-Agrasar, A., & Simal-Gándara, J. (2017). Physico-chemical characterization and evaluation of bio-efficacies of black pepper essential oil encapsulated in hydroxypropyl-beta-cyclodextrin. *Food Hydrocolloids, 65*, 157-164. doi:https://doi.org/10.1016/j.foodhyd.2016.11.014

Raut, J. S., & Karuppayil, S. M. (2014). A status review on the medicinal properties of essential oils. *Industrial Crops and Products, 62*, 250-264. doi:https://doi.org/10.1016/j.indcrop.2014.05.055

Research, G. V. (2018).

Essential Oils Market Size, Share & Trends Analysis Report By Application (Cleaning & Home, Medical, Food & Beverages, Spa & Relaxation), By Product, By Sales Channel, And Segment Forecasts (Research). (978-1-68038-549-6). Retrieved 2019, from Grand View Research https://www.grandviewresearch.com/industry-analysis/essential-oils-market

Ribeiro-Santos, R., Andrade, M., Melo, N. R. d., & Sanches-Silva, A. (2017). Use of essential oils in active food packaging: Recent advances and future trends. *Trends in Food Science & Technology, 61*, 132-140. doi:https://doi.org/10.1016/j.tifs.2016.11.021

Robertson, G. L. (2005). *Food packaging: principles and practice*: CRC press.

Rusa, C. C., Bullions, T. A., Fox, J., Porbeni, F. E., Wang, X., & Tonelli, A. E. (2002). Inclusion Compound Formation with a New Columnar Cyclodextrin Host. *Langmuir, 18*(25), 10016-10023. doi:10.1021/la0262452

Sagiri, S. S., Anis, A., & Pal, K. (2016). Review on Encapsulation of Vegetable Oils: Strategies, Preparation Methods, and Applications. *Polymer-Plastics Technology and Engineering, 55*(3), 291-311. doi:10.1080/03602559.2015.1050521

Santos, E. H., Kamimura, J. A., Hill, L. E., & Gomes, C. L. (2015). Characterization of carvacrol beta-cyclodextrin inclusion complexes as delivery systems for antibacterial and antioxidant applications. *LWT - Food Science and Technology, 60*(1), 583-592. doi:10.1016/j.lwt.2014.08.046

Saokham, P., Muankaew, C., Jansook, P., & Loftsson, T. (2018). Solubility of Cyclodextrins and Drug/Cyclodextrin Complexes. *Molecules (Basel, Switzerland), 23*(5), 1161. doi:10.3390/molecules23051161

Seo, E.-J., Min, S.-G., & Choi, M.-J. (2010). Release characteristics of freeze-dried eugenol encapsulated with β-cyclodextrin by molecular inclusion method. *Journal of Microencapsulation, 27*(6), 496-505. doi:10.3109/02652041003681398

Shan, L., Tao, E.-X., Meng, Q.-H., Hou, W.-X., Liu, K., Shang, H.-C., . . . Zhang, W.-F. (2016). Formulation, optimization, and pharmacodynamic evaluation of chitosan/phospholipid/β-cyclodextrin microspheres. *Drug design, development and therapy, 10*, 417-429. doi:10.2147/DDDT.S97982

Sharifi-Rad, J., Sureda, A., Tenore, C. G., Daglia, M., Sharifi-Rad, M., Valussi, M., . . . Iriti, M. (2017). Biological Activities of Essential Oils: From Plant Chemoecology to Traditional Healing Systems. *Molecules, 22*(1). doi:10.3390/molecules22010070

Sherry, M., Charcosset, C., Fessi, H., & Greige-Gerges, H. (2013). Essential oils encapsulated in liposomes: a review. *Journal of Liposome Research, 23*(4), 268-275. doi:10.3109/08982104.2013.819888

Shin, J., Kathuria, A., & Lee, Y. S. (2019). Effect of hydrophilic and hydrophobic cyclodextrins on the release of encapsulated allyl isothiocyanate (AITC) and their potential application for plastic film extrusion. *Journal of Applied Polymer Science, 136*(42), 48137. doi:10.1002/app.48137

Szejtli, J. (1998). Introduction and General Overview of Cyclodextrin Chemistry. *Chemical Reviews, 98*(5), 1743-1754. doi:10.1021/cr970022c
Topuz, F., & Uyar, T. (2019). Electrospinning of nanocomposite nanofibers from cyclodextrin and laponite. *Composites Communications, 12*, 33-38. doi:https://doi.org/10.1016/j.coco.2018.12.002
Torres-Giner, S. (2011). 5 - Electrospun nanofibers for food packaging applications. In J.-M. Lagarón (Ed.), *Multifunctional and Nanoreinforced Polymers for Food Packaging* (pp. 108-125): Woodhead Publishing.
Torres-Giner, S., Busolo, M., Cherpinski, A., & Lagaron, J. M. (2018). CHAPTER 10 Electrospinning in the Packaging Industry *Electrospinning: From Basic Research to Commercialization* (pp. 238-260): The Royal Society of Chemistry.
Torres-Giner, S., Martinez-Abad, A., & Lagaron, J. M. (2014). Zein-based ultrathin fibers containing ceramic nanofillers obtained by electrospinning. II. Mechanical properties, gas barrier, and sustained release capacity of biocide thymol in multilayer polylactide films. *Journal of Applied Polymer Science, 131*(18), 9270-9276. doi:10.1002/app.40768
Torres-Giner, S., Pérez-Masiá, R., & Lagaron, J. M. (2016). A review on electrospun polymer nanostructures as advanced bioactive platforms. *Polymer Engineering and Science, 56*(5), 500-527. doi:10.1002/pen.24274
Torres-Giner, S., Torres, A., Ferrándiz, M., Fombuena, V., & Balart, R. (2017). Antimicrobial activity of metal cation-exchanged zeolites and their evaluation on injection-molded pieces of bio-based high-density polyethylene. *Journal of Food Safety, 37*, 1-12.
Torres-Giner, S., Wilkanowicz, S., Melendez-Rodriguez, B., & Lagaron, J. M. (2017). Nanoencapsulation of Aloe vera in Synthetic and Naturally Occurring Polymers by Electrohydrodynamic Processing of Interest in Food Technology and Bioactive Packaging. *Journal of Agricultural and Food Chemistry, 65*(22), 4439-4448. doi:10.1021/acs.jafc.7b01393
Wang, C. X., & Chen, S. L. (2005). Fragrance-release Property of β-Cyclodextrin Inclusion Compounds and their Application in Aromatherapy. *Journal of Industrial Textiles, 34*(3), 157-166. doi:10.1177/1528083705049050
Yildiz, Z. I., Celebioglu, A., Kilic, M. E., Durgun, E., & Uyar, T. (2018). Menthol/cyclodextrin inclusion complex nanofibers: Enhanced water-solubility and high-temperature stability of menthol. *Journal of Food Engineering, 224*, 27-36. doi:https://doi.org/10.1016/j.jfoodeng.2017.12.020
Zainuddin, S., Kamrul Hasan, S. M., Loeven, D., & Hosur, M. (2019). Mechanical, Fire Retardant, Water Absorption and Soil Biodegradation Properties of Poly(3-hydroxy-butyrate-co-3-valerate) Nanofilms. *Journal of Polymers and the Environment, 27*(10), 2292-2304. doi:10.1007/s10924-019-01517-9
Zhang, J., Shishatskaya, E. I., Volova, T. G., da Silva, L. F., & Chen, G.-Q. (2018). Polyhydroxyalkanoates (PHA) for therapeutic applications. *Materials Science and Engineering: C, 86*, 144-150. doi:https://doi.org/10.1016/j.msec.2017.12.035
Zhang, M., Wang, J., Lyu, Y., Fitriyanti, M., Hou, H., Jin, Z., . . . Narsimhan, G. (2018). Understanding the antimicrobial activity of water soluble γ-cyclodextrin/alamethicin complex. *Colloids and Surfaces B: Biointerfaces, 172*, 451-458. doi:https://doi.org/10.1016/j.colsurfb.2018.08.065

Table 1
Molecular dimensions and physical properties of α- and γ-cyclodextrins (CDs) (Szejtli, 1998).

Fig. 1. (**a**) Chemical structure and (**b**) the toroidal shape of $\boldsymbol{\alpha}$- and $\boldsymbol{\gamma}$-cyclodextrins (CDs).

Table 2
Encapsulation efficiency (EE,%) and loading capacity (LC,%) values of the α- and γ-cyclodextrin: oregano essential oil inclusion complexes ($\boldsymbol{\alpha}$-CD:OEO and $\boldsymbol{\gamma}$-CD:OEO) by kneading method (KM) and freeze-drying method (FDM).

Fig. 2. Scanning electron microscopy images of (**a**) empty "*as-received*" α-CD (10671x and 1014x), **(a_1)** empty "*kneaded for18 minutes at R.T.* " α-CD (7226x and 696x), **(a_2)** empty "*kneaded for18 minutes with 0.25 mL distilled water at R.T."* α-CD (7546x and 828x); **(b)** α-CD:OEO inclusion complex (10965x and 1313x); **(c)** empty "*as-received*" γ-CD (12152x and 700x), **(c_1)** empty "*kneaded for 18 minutes at R.T.*" γ-CD) (8924x and 776x), **(c_2)** empty "*kneaded for 18 minutes with 0.25 mL distilled water at R.T.*" γ-CD (6979x and 755x); **(d)** γ-CD:OEO inclusion complex (9379x and 1036x).

Fig. 2. Scanning electron microscopy images of **(e)** α-CD:OEO inclusion complex, and **(f)** γ-CD:OEO inclusion complex.

Fig. 2. Scanning electron microscopy images of **(g)** α-CD:oregano essential oil (80:20 w/w, KM) inclusion complex, **(h)** γ-CD:oregano essential oil (80:20 w/w, KM) inclusion complex; (**i**) empty "*as-received*"α- CD and **(j)** empty "*as-received*" γ –CD.

Fig. 3. TEM micrographs of (**a**) 0.1% (w/v) γ-CD:OEO inclusion complex aqueous suspension vortex 10 minutes at 2500 rpm, R.T.; (**$b_{1\text{-}3}$**) 1 % (w/v) γ-CD:OEO inclusion complex aqueous suspension vortex 10 minutes at 2500 rpm, R.T; (**$c_{1\text{-}4}$**) empty "*as-received*" γ- CD aqueous solution vortex 10 minutes at 2500 rpm, R.T.

Fig. 4. X-Ray patterns of (**a**) empty α-CD and α-CD:OEO inclusion complexes, (**b**) empty γ-CD and γ-CD:OEO inclusion complexes (80:20 w/w, KM).

Fig. 5. Scanning electron microscopy micrographs of electrospun fibers of poly(3-hydroxybutyrate-*co*-3-hydroxyvalerate) (PHBV) containing oregano essential oil α- and γ-cyclodextrin inclusion complexes ($\boldsymbol{\alpha}$-CD:OEO and $\boldsymbol{\gamma}$-CD:OEO): (a) 10 wt% **γ**-CD:OEO, (b) 15 wt% **γ**-CD:OEO, (c) 20 wt% **γ**-CD:OEO, (d) 25 wt% **γ**-CD:OEO, (e) 30 wt% **γ**-CD:OEO, (f) 10 wt% **α**-CD:OEO, (g) 15 wt% **α**-CD:OEO, (h) 20 wt% **α**-CD:OEO, (i) 25 wt% **α**-CD:OEO, and (j) 30 wt% **α**-CD:OEO. Scale markers of 10 µm in all cases.

Table 3
Mean diameters and thickness of the electrospun fibers and film thicknesses of poly(3-hydroxybutyrate-*co*-3-hydroxyvalerate) (PHBV) containing oregano essential oil α- and γ-cyclodextrin inclusion complexes ($\boldsymbol{\alpha}$-CD:OEO and $\boldsymbol{\gamma}$-CD:OEO).

Fig. 6. Scanning electron microscopy micrographs of electrospun films of poly(3-hydroxybutyrate-*co*-3-hydroxyvalerate) (PHBV) containing oregano essential oil α-cyclodextrin inclusion complexes (α-CD:OEO): (**a, b**) 10 wt% γ-CD:OEO, (**c, d**) 15 wt% γ-CD:OEO, (**e, f**) 20 wt% γ-CD:OEO, (**g, h**) 25 wt% γ-CD:OEO, and (**i, j**) 30 wt% γ-CD:OEO. Scale markers of 50 µm in all cases.

Fig. 7. Scanning electron microscopy (SEM) micrographs of electrospun films of poly(3-hydroxybutyrate-*co*-3-hydroxyvalerate) (PHBV) containing oregano essential oil α-cyclodextrin inclusion complexes ($\boldsymbol{\alpha}$-CD:OEO): (**a**, **b**) 10 wt% α-CD:OEO, (**c**, **d**) 15 wt% α-CD:OEO, (**e, f**) 20 wt% α-CD:OEO, (**g**, **h**) 25 wt% α-CD:OEO, and (**i**, **j**) 30 wt% α-CD:OEO. Scale markers of 10 µm in all cases. Scale markers of 50 µm in all cases.

Fig. 8. Visual aspect of electrospun films of poly(3-hydroxybutyrate-*co*-3-hydroxyvalerate) (PHBV) containing oregano essential oil α- and γ-cyclodextrin inclusion complexes (α-CD:OEO and γ-CD:OEO). Films are 2 x 2 cm^2.

Fig. 9. Thermogravimetric analysis (TGA) curves for the oregano essential oil α- and γ-cyclodextrin inclusion complexes (α-CD:OEO and γ-CD:OEO) and the electrospun films of poly(3-hydroxybutyrate-*co*-3-hydroxyvalerate) (PHBV) containing γ-CD:OEO and α-CD:OEO inclusion complexes.

Table 4
Thermal properties defined as mass loss at 5% ($T_{5\%}$), mass at 160 ºC, degradation temperature (T_{deg}), weight loss at T_{deg}, and residual mass at 700 ºC for oregano essential oil (OEO), α- and γ-cyclodextrins (α-CD and γ-CD), their inclusion complexes ($\boldsymbol{\alpha}$-CD:OEO and γ-CD:OEO), and the electrospun films of poly(3-hydroxybutyrate-*co*-3-hydroxyvalerate) (PHBV) and PHBV containing γ-CD and α-CD and α-CD:OEO and γ-CD:OEO inclusion complexes.

Table 5
Mechanical properties in terms of elastic modulus ($\boldsymbol{E}$), tensile strength at break ($\boldsymbol{\sigma_b}$), elongation at break ($\boldsymbol{\varepsilon_b}$) for the electrospun films of poly(3-hydroxybutyrate-*co*-3-hydroxyvalerate) (PHBV) and PHBV containing α- and γ-cyclodextrins ($\boldsymbol{\alpha}$-CD and γ-CD) and the oregano essential oil (OEO) inclusion complexes ($\boldsymbol{\alpha}$-CD:OEO and γ-CD:OEO).

Table 6
Minimum inhibitory concentration (MIC) and minimum bactericidal concentration (MBC) of the oregano essential oil α- and γ-cyclodextrin inclusion complexes ($\boldsymbol{\alpha}$-CD:OEO and $\boldsymbol{\gamma}$-CD:OEO) against *S. aureus* and *E. coli*.

Fig. 10. Antimicrobial activity of the electrospun films of poly(3-hydroxybutyrate-*co*-3-hydroxyvalerate) (PHBV) containing 25 wt% oregano essential oil γ-cyclodextrin inclusion complex (γ-CD:OEO) and 15 wt% OEO α-cyclodextrin inclusion complex (α-CD:OEO) in an open and closed system for 15 days against *S. aureus* and *E. coli*.

Fig. 11. Inhibition percentage (%) of 2,2-diphenyl-1-picrylhydrazyl radical (DPPH) for pure oregano essential oil (OEO), oregano essential oil γ- and α-cyclodextrin inclusion complex (γ-CD:OEO and α-CD:OEO) and the electrospun poly(3-hydroxybutyrate-*co*-3-hydroxyvalerate) (PHBV) films containing 25wt% γ-CD:OEO and 15 wt% α-CD:OEO inclusion complexes in an open a closed system for 15 days.

Table 7
Concentration (eq. trolox/g sample) of 2,2-diphenyl-1-picrylhydrazyl radical (DPPH) for the electrospun poly(3-hydroxybutyrate-*co*-3-hydroxyvalerate) (PHBV) films containing 25 wt% oregano essential oil γ-cyclodextrin inclusion complex (γ-CD:OEO) and 15 wt% OEO α-cyclodextrin inclusion complex (α-CD:OEO) in an open a closed system for 15 days.

(a)

(b)

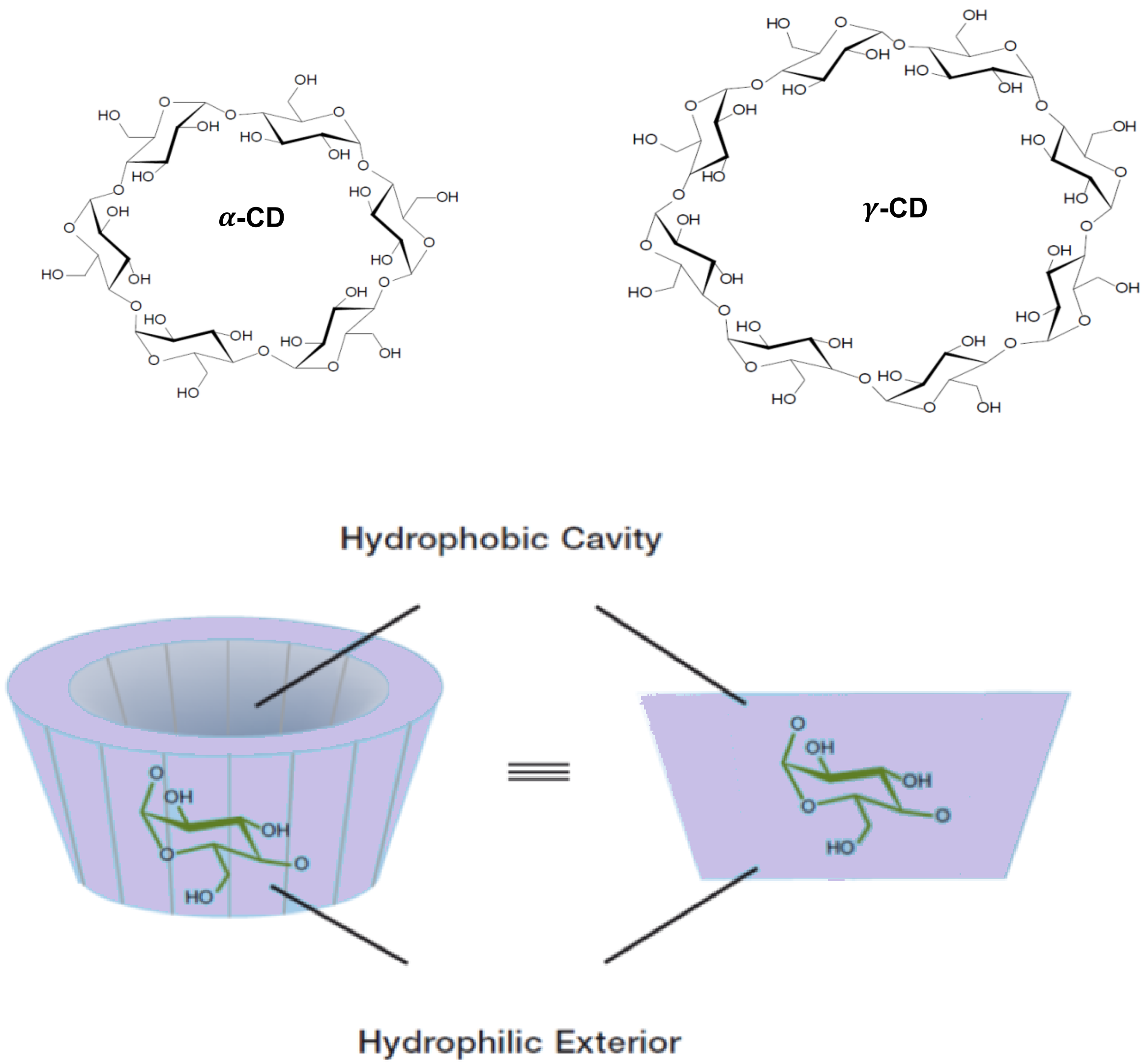

Fig. 1

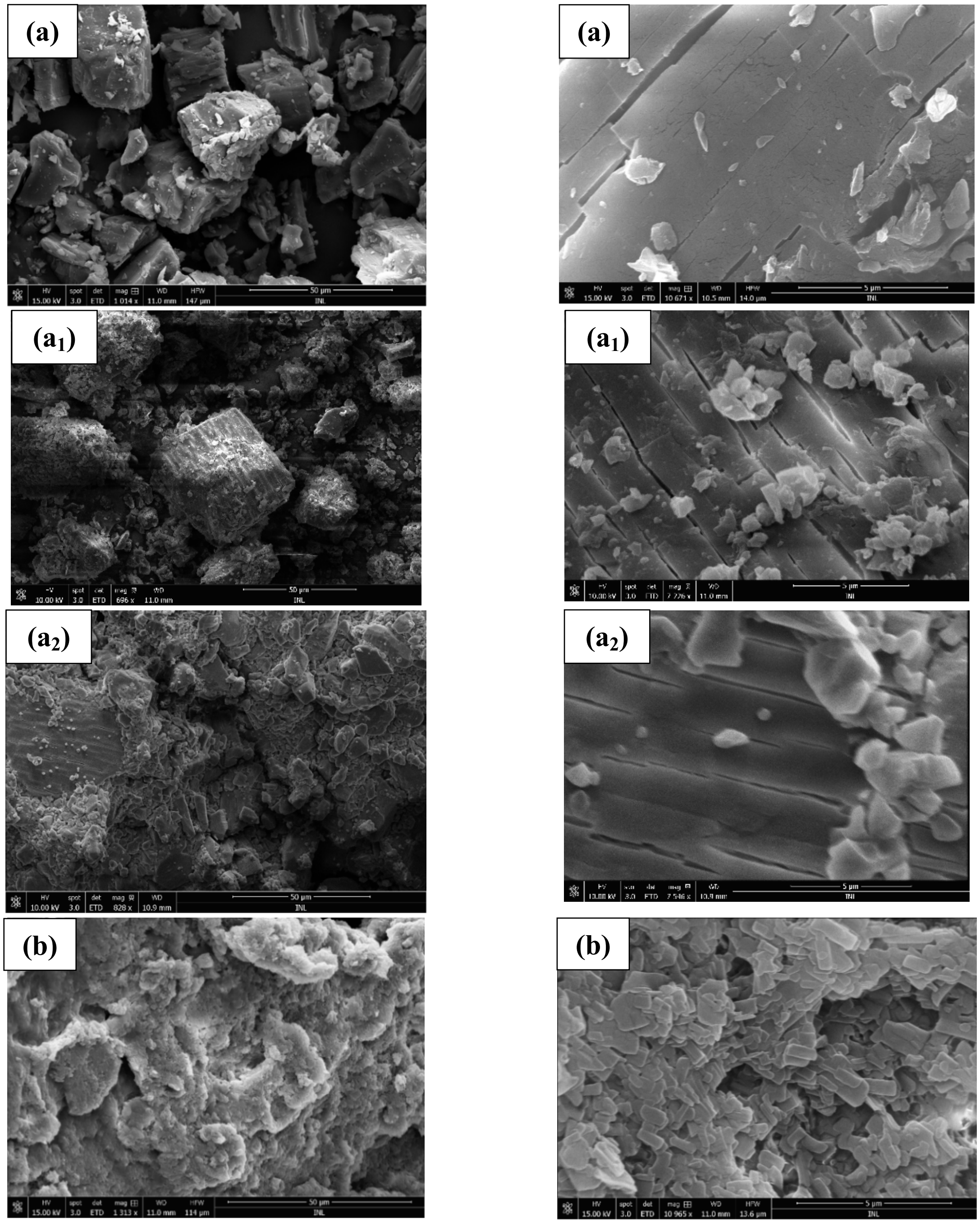
(a)
(a)
(a_1)
(a_1)
(a_2)
(a_2)
(b)
(b)

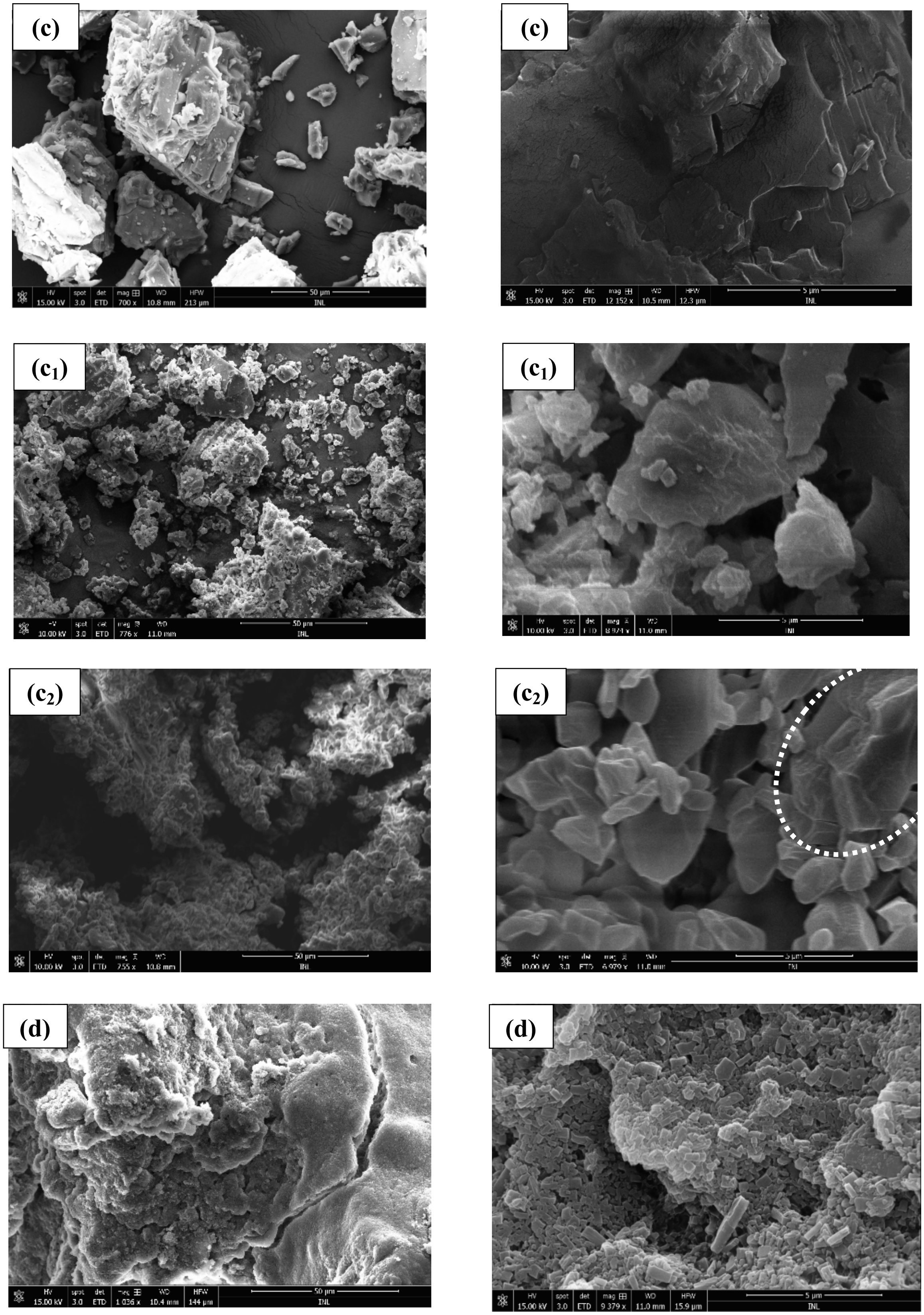

Figs. 2a, 2b, 2c and 2d

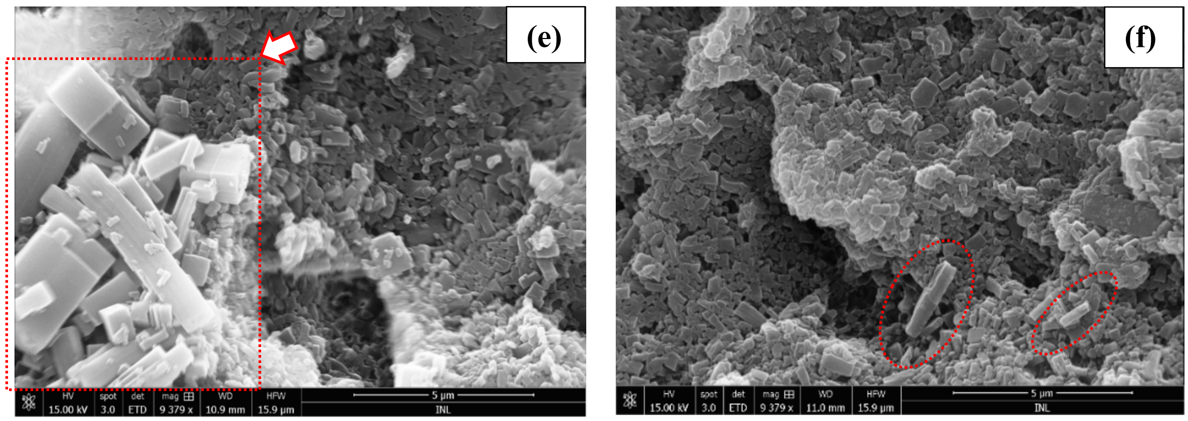

Figs. 2e and 2f

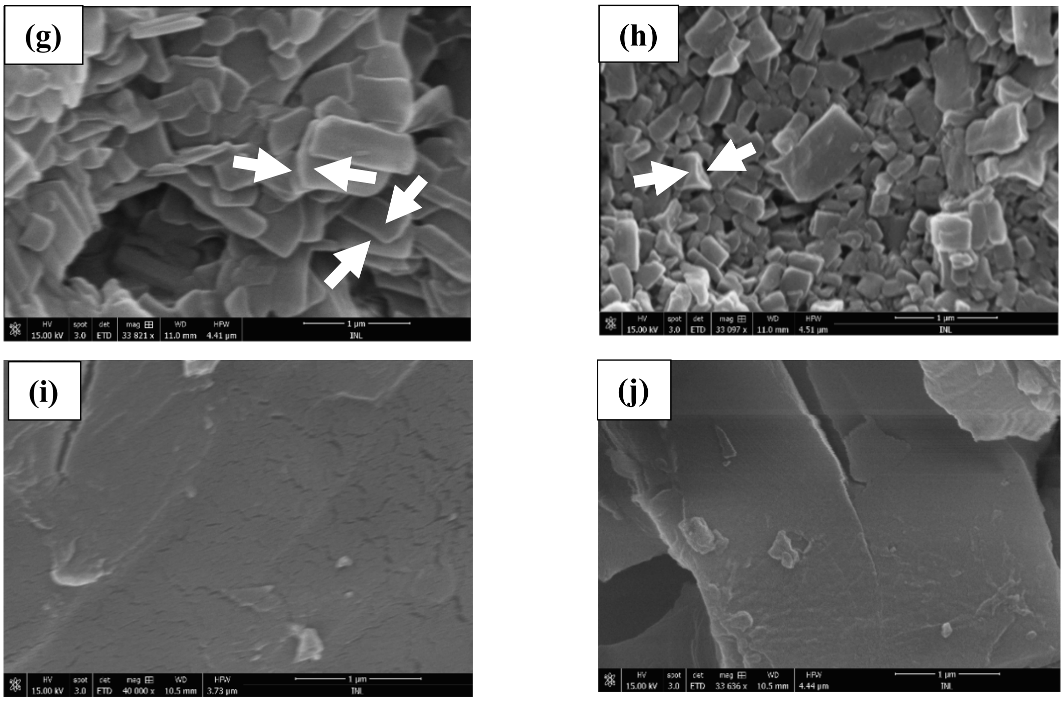

Figs. 2g, 2h, 2i and 2j

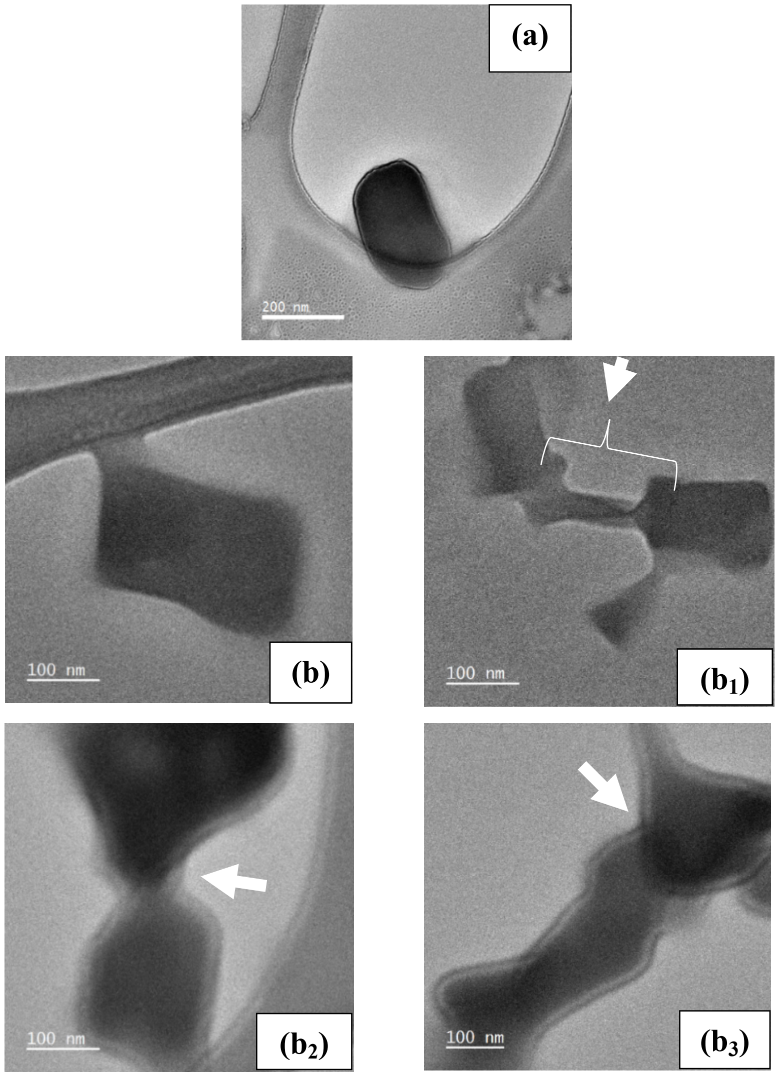

(a)
200 nm
100 nm
(b)
100 nm
(b1)
100 nm
(b2)
100 nm
(b3)

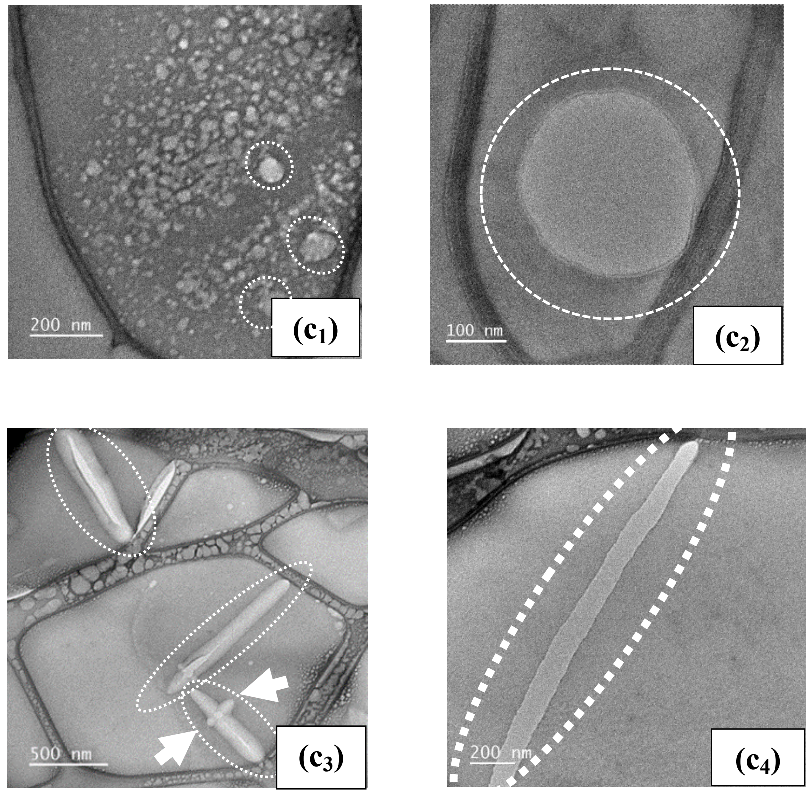

Fig. 3

(a)

(b)

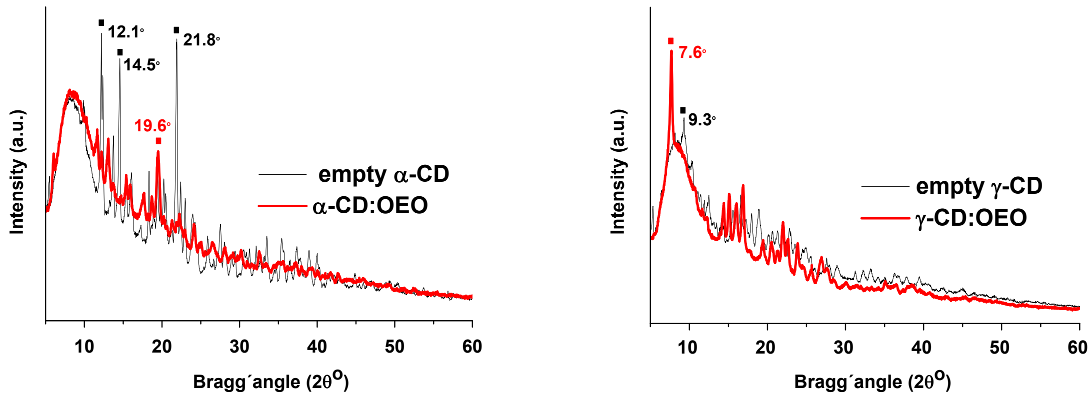

12.1°
14.5°
21.8°
19.6°
empty α-CD
α-CD:OEO
Intensity (a.u.)
Bragg´angle (2θ°)
7.6°
9.3°
empty γ-CD
γ-CD:OEO
Intensity (a.u.)
Bragg´angle (2θ°)

Fig. 4

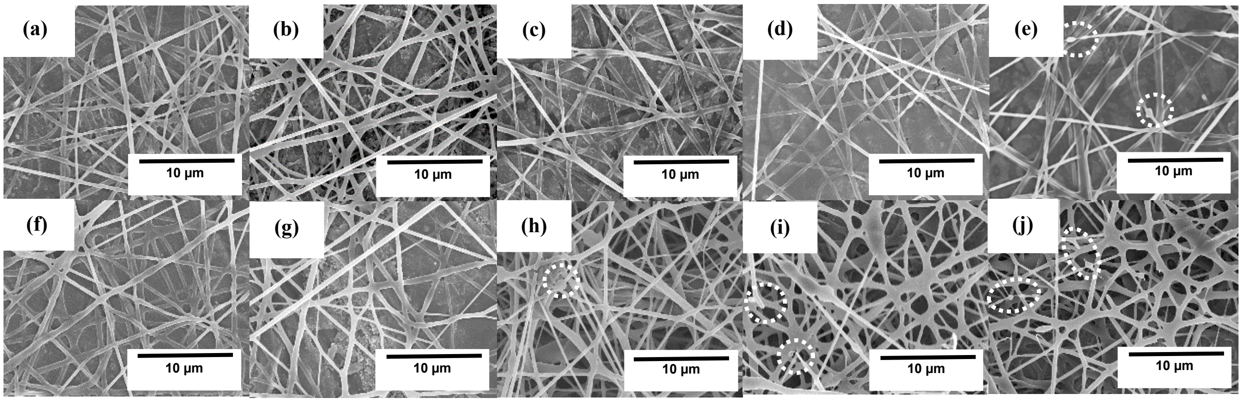
(a)
10 µm
(b)
10 µm
(c)
10 µm
(d)
10 µm
(e)
10 µm
(f)
10 µm
(g)
10 µm
(h)
10 µm
(i)
10 µm
(j)
10 µm

Fig. 5

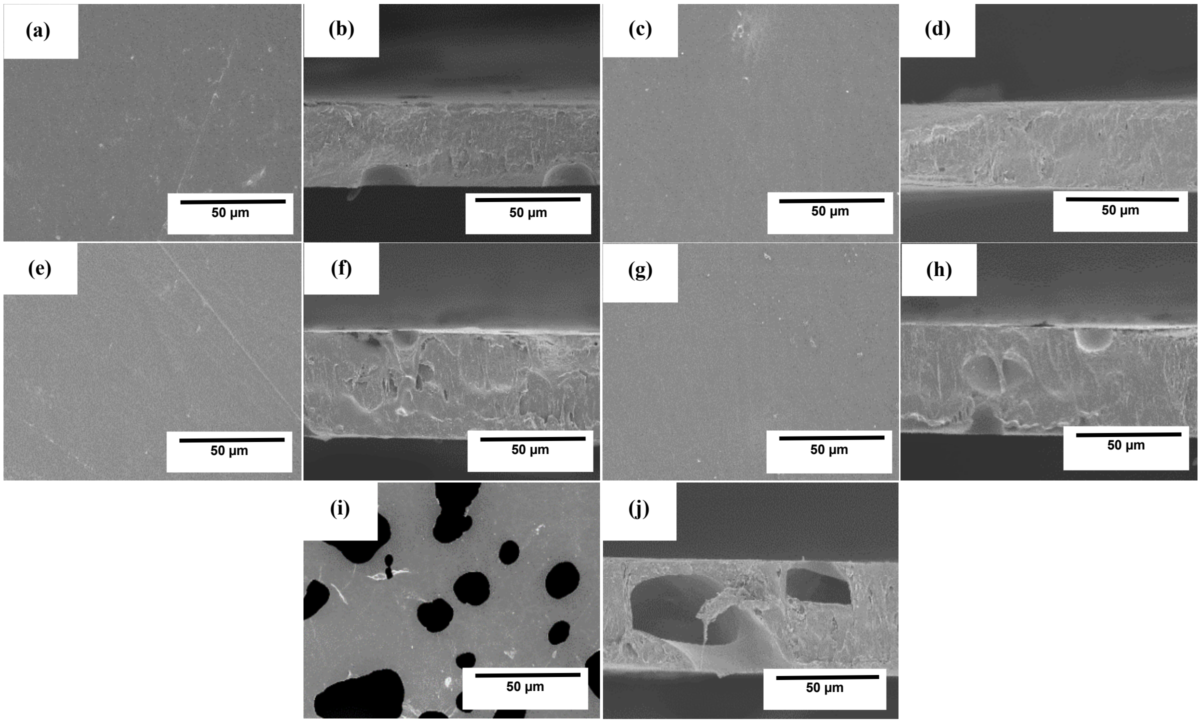
(a)
50 µm
(b)
50 µm
(c)
50 µm
(d)
50 µm
(e)
50 µm
(f)
50 µm
(g)
50 µm
(h)
50 µm
(i)
50 µm
(j)
50 µm

Fig. 6

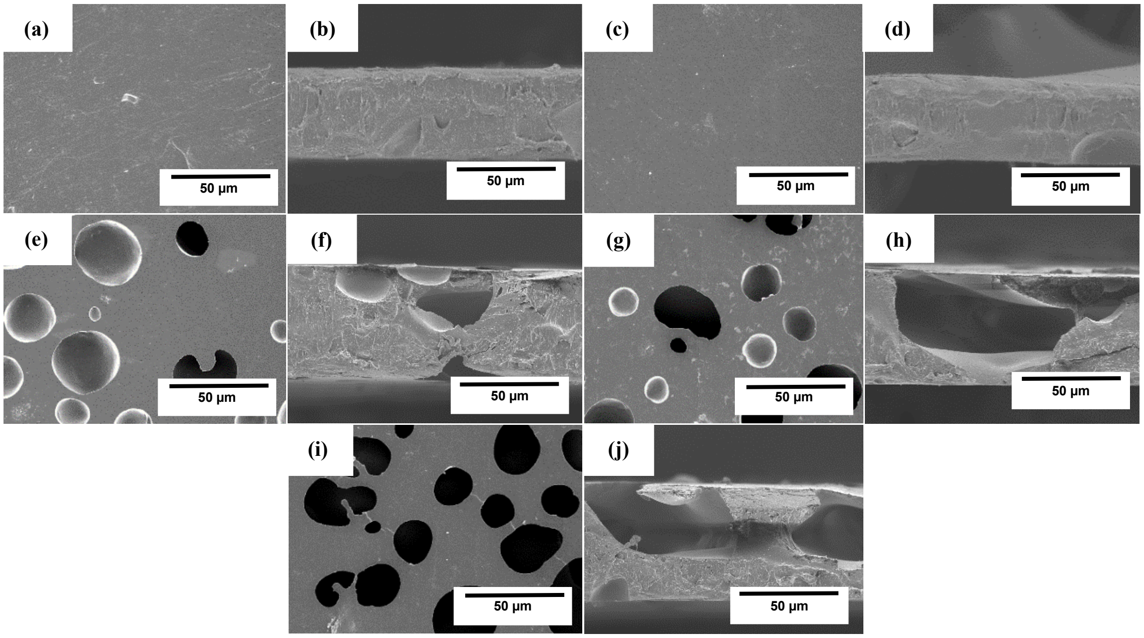
(a)
50 µm
(b)
50 µm
(c)
50 µm
(d)
50 µm
(e)
50 µm
(f)
50 µm
(g)
50 µm
(h)
50 µm
(i)
50 µm
(j)
50 µm

Fig. 7

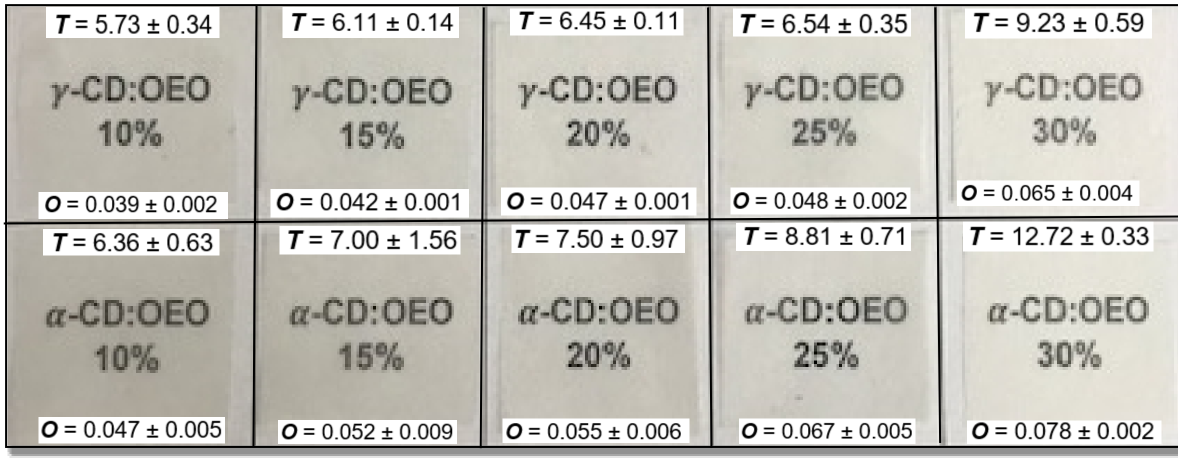

T = 5.73 ± 0.34
γ-CD:OEO
10%
O = 0.039 ± 0.002
T = 6.11 ± 0.14
γ-CD:OEO
15%
O = 0.042 ± 0.001
T = 6.45 ± 0.11
γ-CD:OEO
20%
O = 0.047 ± 0.001
T = 6.54 ± 0.35
γ-CD:OEO
25%
O = 0.048 ± 0.002
T = 9.23 ± 0.59
γ-CD:OEO
30%
O = 0.065 ± 0.004
T = 6.36 ± 0.63
α-CD:OEO
10%
O = 0.047 ± 0.005
T = 7.00 ± 1.56
α-CD:OEO
15%
O = 0.052 ± 0.009
T = 7.50 ± 0.97
α-CD:OEO
20%
O = 0.055 ± 0.006
T = 8.81 ± 0.71
α-CD:OEO
25%
O = 0.067 ± 0.005
T = 12.72 ± 0.33
α-CD:OEO
30%
O = 0.078 ± 0.002

Fig. 8

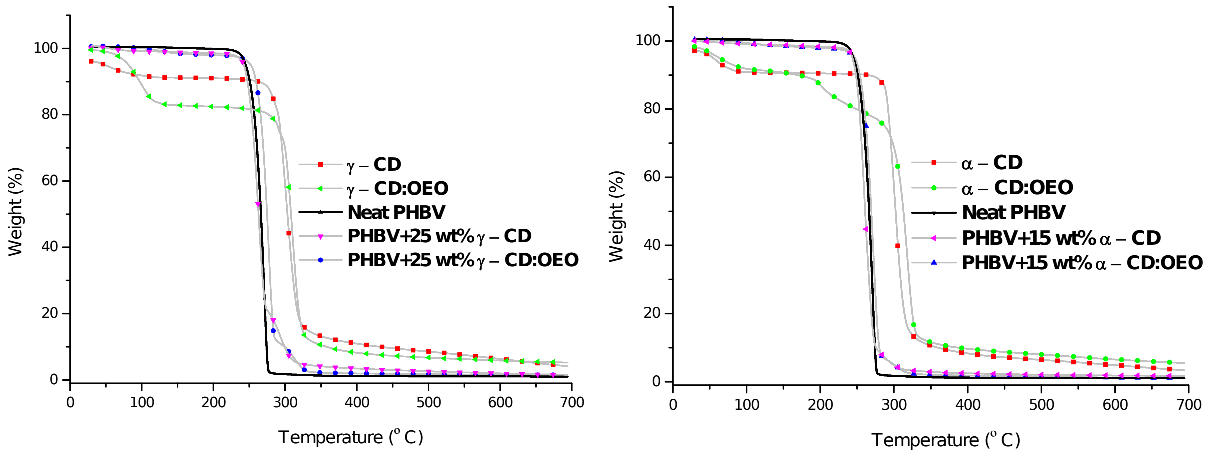

Weight (%)
Temperature (°C)
γ – CD
γ – CD:OEO
Neat PHBV
PHBV+25 wt% γ – CD
PHBV+25 wt% γ – CD:OEO
α – CD
α – CD:OEO
Neat PHBV
PHBV+15 wt% α – CD
PHBV+15 wt% α – CD:OEO

Fig. 9

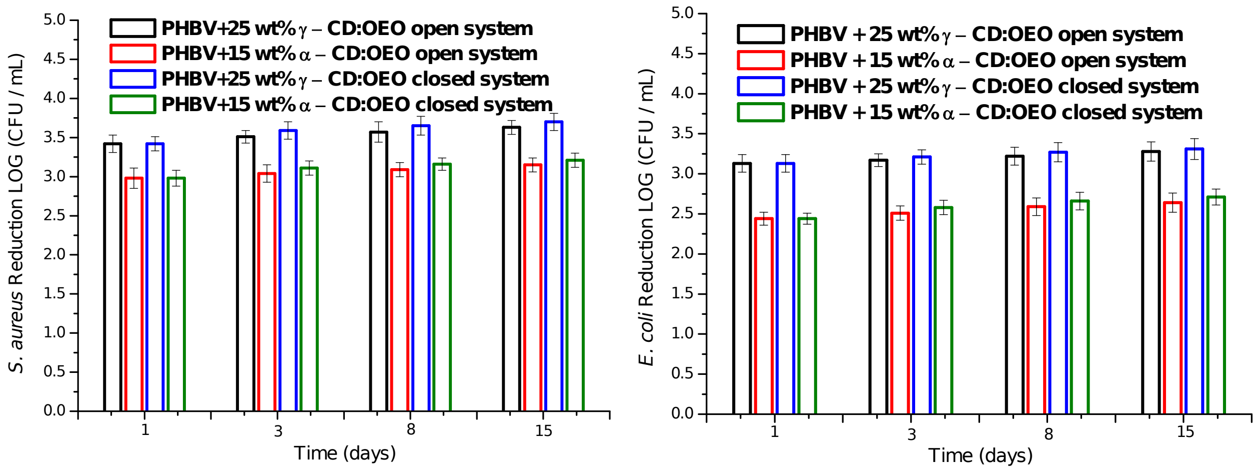
PHBV+25 wt% γ – CD:OEO open system
PHBV+15 wt% α – CD:OEO open system
PHBV+25 wt% γ – CD:OEO closed system
PHBV+15 wt% α – CD:OEO closed system
S. aureus Reduction LOG (CFU / mL)
Time (days)
E. coli Reduction LOG (CFU / mL)
1
3
8
15
0.0
0.5
1.0
1.5
2.0
2.5
3.0
3.5
4.0
4.5
5.0

Fig. 10

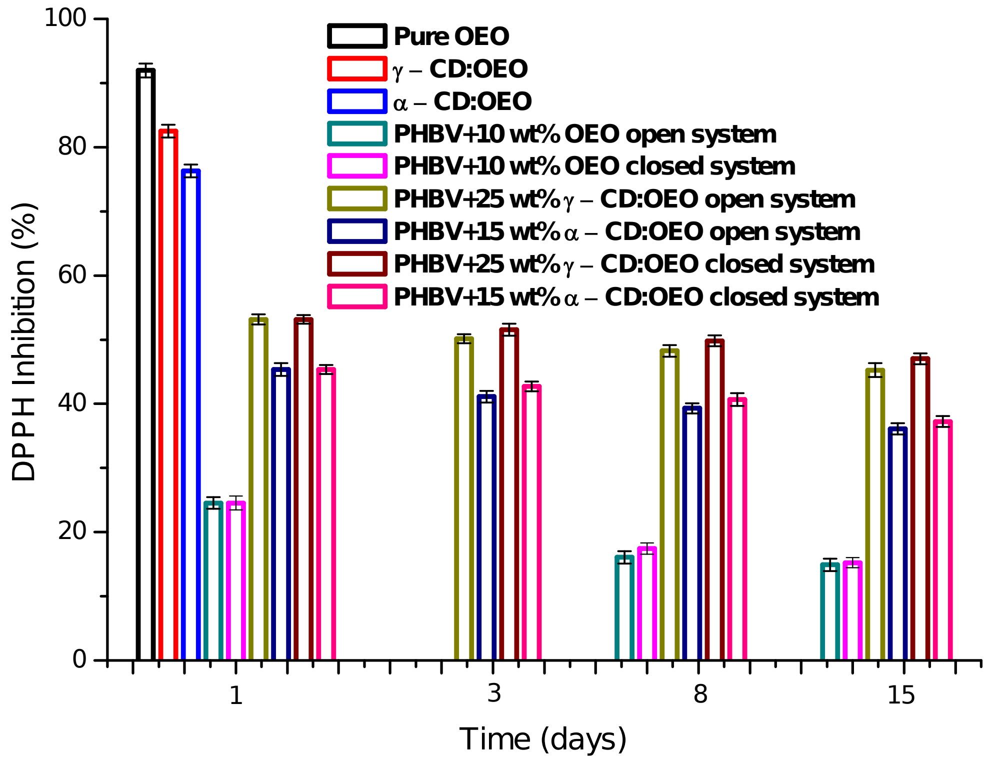
Pure OEO
γ – CD:OEO
α – CD:OEO
PHBV+10 wt% OEO open system
PHBV+10 wt% OEO closed system
PHBV+25 wt% γ – CD:OEO open system
PHBV+15 wt% α – CD:OEO open system
PHBV+25 wt% γ – CD:OEO closed system
PHBV+15 wt% α – CD:OEO closed system
DPPH Inhibition (%)
0
20
40
60
80
100
1
3
8
15
Time (days)

Fig. 11

Table 1

Molecular dimensions and physical properties of α- and γ-cyclodextrins (CDs) (Szejtli, 1998).

CD	No of Glucose units	Molecular weight (g/mol)	Molecular Dimensions (Å)			Solubility at 25 ºC (g/100 mL H_2O)
			Inside diameter	Outside diameter	Height	
$\boldsymbol{\alpha}$	6	973	5.7	13.7	7.0	14.50
$\boldsymbol{\gamma}$	8	1297	9.5	16.9	7.0	23.20

Table 2

Encapsulation efficiency (EE,%) and loading capacity (LC,%) values of the α- and γ-cyclodextrin: oregano essential oil inclusion complexes (**α**-CD:OEO and **γ**-CD:OEO) by kneading method (KM) and freeze-drying method (FDM).

Method	**Inclusion Complex**	**EE (%)***	**LC (%)***
KM	γ-CD:OEO 80: 20 w/w	98.50 ± 0.7^{a}	19.60 ± 0.1^{a}
	α-CD:OEO 80: 20 w/w	92.60 ± 3.6^{a}	18.60 ± 0.7^{a}
	γ-CD:OEO 85: 15 w/w	71.20 ± 6.5^{a}	10.80 ± 1.0^{a}
	α-CD:OEO 85: 15 w/w	96.20 ± 1.4^{a}	14.40 ± 0.2^{a}
FDM	γ-CD:OEO 80: 20 w/w	93.60 ± 2.5^{b}	18.70 ± 0.5^{b}
	α-CD:OEO 80: 20 w/w	36.03 ± 1.2^{b}	7.20 ± 0.2^{b}
	γ-CD:OEO 85: 15 w/w	96.70 ± 0.6^{b}	14.50 ± 0.1^{b}
	α-CD:OEO 85: 15 w/w	50.02 ± 2.6^{b}	7.50 ± 0.4^{b}

*Values given are averages of triplicate samples ± standard deviations. Average values with different superscript letters differ statistically (*p*□0.05); (a and b: indicate statistically difference among formulations KM *vs* FDM, values followed by the same letter are not statistically different according to Tukey's Multiple Range Test).

Table 3

Mean diameters and thickness of the electrospun fibers and film thicknesses of poly(3-hydroxybutyrate-*co*-3-hydroxyvalerate) (PHBV) containing oregano essential oil α- and γ-cyclodextrin inclusion complexes ($\boldsymbol{\alpha}$-CD:OEO and $\boldsymbol{\gamma}$-CD:OEO).

Sample	Fiber diameter (µm)	Film thickness (µm)
PHBV	0.89 ± 0.30	64 ± 0.75
PHBV + 10 wt% $\boldsymbol{\gamma}$-CD:OEO	0.87 ± 0.15	61 ± 1.10
PHBV + 15 wt% $\boldsymbol{\gamma}$-CD:OEO	0.88 ± 0.22	63 ± 0.98
PHBV + 20 wt% $\boldsymbol{\gamma}$-CD:OEO	0.86 ± 0.18	70 ± 0.94
PHBV + 25 wt% $\boldsymbol{\gamma}$-CD:OEO	0.85 ± 0.27	72 ± 0.72
PHBV + 30 wt% $\boldsymbol{\gamma}$-CD:OEO	0.91± 0.32	77 ± 0.68
PHBV + 10 wt% $\boldsymbol{\alpha}$-CD:OEO	0.89 ± 0.20	73 ± 0.99
PHBV + 15 wt% $\boldsymbol{\alpha}$-CD:OEO	0.90 ± 0.17	75 ± 0.77
PHBV + 20 wt% $\boldsymbol{\alpha}$-CD:OEO	1.03 ± 0.25	81 ± 0.91
PHBV + 25 wt% $\boldsymbol{\alpha}$-CD:OEO	1.17 ± 0.19	83 ± 0.86
PHBV + 30 wt% $\boldsymbol{\alpha}$-CD:OEO	1.22 ± 0.12	85 ± 0.69

Table 4

Thermal properties defined as mass loss at 5% ($T_{5\%}$), mass at 160 ºC, degradation temperature (T_{deg}), weight loss at T_{deg}, and residual mass at 700 ºC for oregano essential oil (OEO), α- and γ-cyclodextrins (α-CD and γ-CD), their inclusion complexes (α-CD:OEO and γ-CD:OEO), and the electrospun films of poly(3-hydroxybutyrate-*co*-3-hydroxyvalerate) (PHBV) and PHBV containing γ-CD and α-CD and α-CD:OEO and γ-CD:OEO inclusion complexes.

Sample	$T_{5\%}$ (ºC)	Mass at 160ºC (%)	T_{deg} (ºC)	Mass loss (%)	Residual mass (%)
PHBV	245.03	0.15	278.70	97.73	2.10
OEO	46.26	40.3	178.40	74.16	0.14
γ-CD	49.23	8.86	323.12	83.01	4.15
α-CD	55.21	9.42	326.43	86.39	3.38
γ-CD:OEO	81.60	16.9	326.28	86.11	5.23
α-CD:OEO	62.97	9.63	330.50	85.70	5.51
PHBV + 25 wt% γ-CD	240.95	1.21	320.11	95.13	1.56
PHBV + 25 wt% γ-CD:OEO	252.02	1.71	322.52	96.12	1.48
PHBV + 15 wt% α-CD	241.55	1.31	309.27	96.28	1.71
PHBV + 15 wt% α-CD:OEO	247.23	1.63	313.70	96.98	1.11

Table 5

Mechanical properties in terms of elastic modulus ($\boldsymbol{E}$), tensile strength at break ($\boldsymbol{\sigma_b}$), elongation at break ($\boldsymbol{\varepsilon_b}$) for the electrospun films of poly(3-hydroxybutyrate-*co*-3-hydroxyvalerate) (PHBV) and PHBV containing α- and γ-cyclodextrins ($\boldsymbol{\alpha}$-CD and $\boldsymbol{\gamma}$-CD) and the oregano essential oil (OEO) inclusion complexes ($\boldsymbol{\alpha}$-CD:OEO and $\boldsymbol{\gamma}$-CD:OEO).

Sample	E (MPa)	σ_b(MPa)	ε_b(%)
Neat PHBV	1252 ± 79[a]	18.1 ± 2.1[a]	2.4 ± 0.3[a]
PHBV + 25 wt% γ-CD	1692 ± 434[b]	9.04 ± 4.2[b]	0.78 ± 0.3[b]
PHBV + 25 wt% γ-CD:OEO	1472 ± 136[c]	9.83 ± 0.8[b]	1.25 ± 0.2[c]
PHBV + 15 wt% α-CD	1594 ± 260[d]	9.10 ± 2.5[b]	0.95 ± 0.3[d]
PHBV + 15 wt% α-CD:OEO	1698 ± 764[b]	9.77 ± 4.6[b]	0.85 ± 2.6[e]

a–e Different letters in the same column indicate a significant difference ($p < 0.05$).

Table 6

Minimum inhibitory concentration (MIC) and minimum bactericidal concentration (MBC) of the oregano essential oil α- and γ-cyclodextrin inclusion complexes (α-CD:OEO and γ-CD:OEO) against *S. aureus* and *E. coli*.

Sample	Microorganism	MIC	MBC
γ-CD:OEO	*E. coli*	0.078 µg/mL	0.078 µg/mL
	S. aureus	0.039 µg/mL	0.039 µg/mL
α-CD:OEO	*E. coli*	0.156 µg/mL	0.156 µg/mL
	S. aureus	0.078 µg/mL	0.078 µg/mL

Table 7

Concentration (eq. trolox/g sample) of 2,2-diphenyl-1-picrylhydrazyl radical (DPPH) for the electrospun poly(3-hydroxybutyrate-*co*-3-hydroxyvalerate) (PHBV) films containing 25 wt% oregano essential oil γ-cyclodextrin inclusion complex (γ-CD:OEO) and 15 wt% OEO α-cyclodextrin inclusion complex (α-CD:OEO) in an open a closed system for 15 days.

Sample	Day	Open system	Closed system
		Eq. trolox/g sample) of DPPH	Eq. trolox/g sample) of DPPH
Pure OEO	1	91.96 ± 0.03^{a}	---
γ-CD:OEO	1	82.51 ± 0.06^{b}	---
α-CD:OEO	1	76.32 ± 0.22^{c}	---
PHBV + 10 wt% OEO	1	26.48 ± 0.04^{d}	26.48 ± 0.04^{d}
	8	16.82 ± 0.09^{e}	17.57 ± 0.04^{e}
	15	15.75 ± 0.06^{e}	16.47 ± 0.01^{e}
PHBV + 25 wt% γ-CD:OEO	1	57.40 ± 0.07^{f}	57.40 ± 0.07^{f}
	3	53.24 ± 0.17^{g}	56.03 ± 0.09^{f}
	8	51.42 ± 0.17^{g}	52.95 ± 0.09^{g}
	15	48.17 ± 0.09^{h}	49.95 ± 0.51^{h}
PHBV + 15 wt% α-CD:OEO	1	47.48 ± 0.07^{h}	47.48 ± 0.07^{h,i}
	3	41.86 ± 0.09^{i}	45.89 ± 0.58^{i}
	8	40.13 ± 0.08^{i}	42.91 ± 0.17^{i,j}
	15	38.42 ± 0.09^{i}	39.26 ± 0.17^{j}

Means ± S.D.

$^{a-j}$ Different letters indicate a significant difference among the samples ($p < 0.05$).

Declaration of interests

X The authors declare that they have no known competing financial interests or personal relationships that could have appeared to influence the work reported in this paper.

☐The authors declare the following financial interests/personal relationships which may be considered as potential competing interests:

DEnescu
29 January 2020